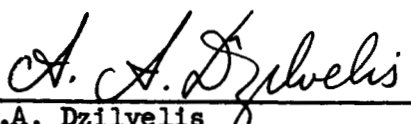


PERFORMANCE ANALYSIS OF THE GENERAL
TWO-BURN GUIDANCE EQUATIONS

18 November 1965

Contract NAS 3-3231


R.C. Eberhard

Approved: 
A.A. Dzilvelis

TRW Systems
One Space Park
Redondo Beach, Calif.

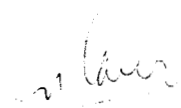


TABLE OF CONTENTS

	Page
1. INTRODUCTION	1
1.1 Objectives of the Performance Analysis	1
1.2 Scope of the Analysis	1
1.3 Performance Analysis Plan	1
2. SUMMARY OF RESULTS	2
2.1 Performance Results	2
2.2 Major Disturbances	3
2.3 Equation Weaknesses	4
3. METHOD OF ANALYSIS	4
3.1 Simulation Program	5
3.1.1 Guidance Equations	5
3.1.2 Vehicle Dynamics Simulation	5
3.1.3 Control System Simulation	6
3.2 Determination of the Reference Trajectory	6
3.3 Disturbance and Dispersions	6
4. APPROXIMATIONS IN THE STUDY	7
4.1 Vehicle Model Approximations	7
4.2 Trajectory Approximations	7
4.3 Guidance Equation Approximations	7
4.3.1 Control System	7
4.3.2 Computation Step Size	8
4.3.3 Signator Simulation	8
4.3.4 IMU Simulation	8
4.3.5 Deviations from GD/C Guidance Equations	8
4.3.5.1 Initial Computations	8
4.3.5.2 Navigation Computations	9
4.3.5.3 Coordinate System and Phase Branch	9
4.3.5.4 Booster Phase	9

	Page
4.3.5.5 Sustainer Phase	9
4.3.5.6 Centaur First Burn Phase	9
4.3.5.7 Parking Orbit	9
4.3.5.8 Centaur Second Burn	10
4.3.5.9 Post Injection Phase	10
4.3.5.10 Cutoff Routine	10
4.3.5.11 Steering Subroutine	10
5. PERFORMANCE CRITERIA	10
5.1 Figure-of-Merit	10
5.2 Impact Criteria	11
5.3 Final Injection Criteria	11
5.4 Parking Orbit Cutoff	12
5.5 Parking Orbit Injection	12
6. GUIDANCE CONSTANTS	12
7. PERTURBATIONS	15
7.1 Parking Orbit Perturbations	15
7.2 Composite Perturbations	15
8. RESULTS OF THE PERFORMANCE ANALYSIS	16
8.1 The Complete Performance Analysis	17
8.1.1 Atmospheric Heating Dispersions	17
8.1.2 Parking Orbit Perigee	17
8.1.3 Parking Orbit Cutoff	17
8.1.4 Final Injection Altitude and Perigee	18
8.1.5 Final Injection Range	18
8.1.6 Final Injection Vis-Viva Energy	18
8.1.7 Final Injection Vehicle Weight	19
8.1.8 Impact Time of Arrival	19
8.1.9 Impact Velocity	20
8.1.10 Impact Miss	20
8.1.11 Figure-of-Merit	20

	Page
8.2 Comparison of Results to GD/C Performance Analysis	21
8.3 Launch Window Study	22
9. CONCLUSIONS AND RECOMMENDATIONS	37
9.1 Conclusions	37
9.2 Recommendations	37
APPENDICES	
A. REFERENCE TRAJECTORY	A-1
B. VEHICLE MODEL	B-1
C. TWO-BURN GUIDANCE EQUATION FLOW CHARTS	C-1
REFERENCES	R-1

1. INTRODUCTION

This report prepared by TRW Systems Group presents the results of a continuing performance analysis of the GD/C developed inflight guidance equations for the Atlas/Centaur Two-Burn flight test missions. TRW Systems performed the study during the period of February to August, 1965.

This report is based primarily on the equations proposed in GD/C's April, 1965, preliminary report on the Two-Burn guidance equations (Reference 1), but the simulation was updated several times in accordance with equation flow charts received from GD/C (Reference 3). The guidance constants are almost all from Reference 1. This analysis follows a similar effort of a more preliminary nature performed a year ago. At that time several deficiencies were found with the Two-Burn equations since they were still in a formative stage. The present analysis however, covers equations which can be considered reasonably up-to-date.

1.1 Objectives of the Performance Analysis

The primary purpose of this performance analysis is to provide an independent verification of the Two-Burn guidance equations for injecting the Atlas/Centaur vehicle into a satisfactory lunar trajectory. Subsidiary objectives are:

- 1) Identify the major sources of performance degradation in the guidance equations.
- 2) Determine which perturbations to the mean vehicle characteristics and environment have the greatest effect on guidance system accuracy.
- 3) Make a rough comparison of the dispersions obtained from selected perturbations to the dispersions found by GD/C and presented in Reference 1.

1.2 Scope of the Analysis

The AC-8 vehicle test flight will be the first Atlas/Centaur flight to use Two-Burn guidance equations to guide the vehicle into a pseudo lunar trajectory. This mission requires that the Centaur vehicle and a dynamic model of the Surveyor spacecraft be injected into a circular parking orbit. The parking orbit for AC-8 will be for a fixed time period after which the Centaur engines will be reignited and the vehicle guided into a pseudo lunar trajectory. Since the same or similar equations will be used for the AC-9 and AC-12 flights with actual Surveyor spacecraft and

actual lunar impacts, this analysis included the guidance controlled variable length parking orbit.

1.3 Performance Analysis Plan

The first step in the performance analysis plan was the development of the digital simulations of the Atlas/Centaur vehicle dynamics and the guidance equations. The second step was to "fly" the guidance equations "piggy back" on an open loop reference trajectory until most of the programming errors had been corrected. The final step was to close the guidance loop and allow the guidance constants to fly the vehicle to lunar impact. This was then called the nominal trajectory and used as a reference in studying the dispersions caused by various disturbances such as variations in thrust, vehicle weight, and control parameters. From the tabulation results a determination was made of the capability of the guidance equations to achieve an acceptable burnout when disturbances were present.

2. SUMMARY OF RESULTS

The overall performance of the Two-Burn equations and constants was, with the exception of the heating parameter, satisfactory and will probably meet a specification similar to that for AC-7 (Reference 2). If significant perturbations are likely to occur in the parking orbit thrust, the performance will be questionable.

2.1 Performance Results

The performance results are given in Table 2.1 for 26 positive perturbation and 25 negative perturbations.

The nominal value of the heating parameter plus the average dispersion rss's add up to 127,967,220 lb/ft which is so close to the 3σ limit for heating that no allowance can be made for targeting, computational or hardware effects.

The parking orbit perigee dispersion shows the excellent control obtained with the continuous altitude control function used. Control of the altitude at parking orbit injection automatically results in control of the altitude of final injection.

The range dispersions rss is large but this is chiefly caused by the coarseness of the parking orbit cutoff which used a sample time of 2 seconds. Better control will be obtained in actual practice.

The weight and impact dispersions rss's are similar to those obtained by TRW for AC-6 and AC-7. The primary cause of impact errors was found to be dispersions in the navigation errors.

Table 2.1
Total Dispersion RSS

Parameters	+ Perturbations	- Perturbations
Heating Parameter	23,428,000 lb/ft	17,252,000 lb/ft
Parking Orbit Perigee	9,638 ft	8,621 ft
Injection Altitude	5,854 ft	4,859 ft
Injection Range	121,526 ft	102,854 ft
Injection Perigee	2,370 ft	1,999 ft
Injection Weight	127 lb	147 lb
Time of Impact	132 sec	116 sec
Impact Velocity	0.500 m/sec	0.438 m/sec
Impact Latitude	0.419 deg	0.477 deg
Impact Longitude	1.850	1.641 deg
Miss Only FOM	0.386 m/sec	0.354 m/sec
Miss Plus Time FOM	1.141 m/sec	1.030 m/sec

2.2 Major Disturbances

Based on the dispersions obtained during this study (and in particular on the payload and FOM dispersions), the 10 most serious perturbations in order of their significance are:

Perturbation	Δ Weight	FOM
Centaur I _{sp}	92.1 lb	.270 m/s
Tailwind	+ 71.0 lb	.271 m/s
Booster I _{sp}	46.9 lb	.149 m/s
Headwind	- 24.7 lb	.450 m/s
Sustainer I _{sp}	29.4 lb	.387 m/s
Fuel Tanking	25.7 lb	.310 m/s
Booster Pitch Program	28.6 lb	.238 m/s
Centaur Weight	29.2 lb	.222 m/s
Sust. Jet Weight	27.7 lb	.240 m/s
Booster Thrust	15.2 lb	.258 m/s

Overshadowing all of these in potential sensitivity is the parking orbit thrust perturbation. Until a magnitude for this perturbation is agreed to however, its true relative significance cannot be established. The primary causes of excessive heating are the booster pitch program and atmospheric density dispersions.

2.3 Equation Weaknesses

Although the latest version of the Two-Burn guidance equations are vastly improved from those examined a year ago some problems still exist.

The excessive heating is not basically a guidance equation problem but a problem with the booster pitch program.

The major weakness of the present equations is their inability to accept acceleration inputs in the parking orbit. Although this is not a design weakness (they were designed to do this), it will cause significant impact errors.

The large magnitudes of the navigation errors encountered in a Two-Burn mission are a weakness for which no obvious cure is available. Although the navigation errors themselves are not particularly sensitive to the perturbations, their large magnitude causes the resultant dispersions in the errors to be significant and cause appreciable time-of-flight errors.

Some difficulty was encountered in obtaining smooth operation from the yaw steering around the antipode. This was due in part to the use of the energy-to-be-gained which is switched near the antipode and partly to unfitted gains.

One logic problem involves the 120 second delay after MECO 1 prior to switching to the parking orbit navigation equations. A certain time period is required for the 100 lb ullage rocket thrust. This is the basic purpose of the 120 second delay. However, the minimum parking orbit time of 2 minutes cannot be met without risking exiting the parking orbit navigation equations without entering them. This would remove the sigmator components of position and velocity destroying the navigation. GD/C is aware of the possibility and has several ways of correcting it depending on how the parking orbit thrust profile is finally settled.

3. METHOD OF ANALYSIS

The approach used for the performance analysis of the Two-Burn guidance equations is described in this section. Sufficient details are provided to judge the validity of the conclusions.

3.1 Simulation Program

The analysis of the performance of a set of guidance equations requires a complex simulation composed of several subroutines. A functional description of the three major subroutines follows.

3.1.1 Guidance Equations

The guidance equations to be studied are programmed for simulation on a general purpose digital computer. The type of simulation used in this analysis is called a "hardware" simulation meaning that the guidance equations are used in almost the same codeable flow-chart form as would be used for programming the flight computer. However, the exact cycle times, scale factors, word lengths, etc., are not duplicated; instead the full capabilities of a general purpose computer are used. Interfaces for steering controls, discrete outputs and the velocity and attitude inputs are included in the simulation.

The "hardware" simulation used in this performance analysis was based on the guidance equations and flow charts presented in Appendix C. These equations were programmed for the IBM 7094 computer to be used in conjunction with the vehicle dynamics simulation.

3.1.2 Vehicle Dynamics Simulation

This program simulates all of the known forces acting on the vehicle and integrates the resulting accelerations to obtain the vehicle's position and velocity. It requires detailed models and data describing the physical characteristics of the vehicle as well as its environment.

Examples of the data necessary are those related to the latest NASA gravitational model and fundamental constants, the Patrick AFB atmospheric model to 300,000 ft. altitude, the vehicle propulsion system models, the vehicle aerodynamic characteristics, planetary ephemeris data, etc.

This program known as the "SNS Program" simulates very accurately the true motion of the missile and spacecraft from the time of launch until lunar impact. Much of the data used to represent the vehicle configurations were not used because of an attempt to remain compatible with the guidance constants obtained from GD/C, which were derived with a simplified vehicle model.

3.1.3 Control System Simulation

In order to simulate the dynamics response lags of the vehicle to guidance steering commands, a simple autopilot model was devised. This model compares the existing vehicle attitude to the desired attitude and generates a steering signal proportional to the angular difference.

3.2 Determination of the Reference Trajectory

The simulation subroutines are combined into one program which with the proper guidance constants and launch conditions will simulate a nominal flight of the vehicle to a lunar impact. The normal method for obtaining the correct constants is to first fly the vehicle dynamics simulation without guidance control using a fixed pitch program for steering control. The launch time, launch azimuth and pitch rates are then adjusted until the desired impact is achieved. Then the guidance is added in an open loop mode to determine the guidance values of position and velocity which include the truncation and gravity model errors. From this data many of the guidance constants can be found analytically. The remaining guidance constants are found by iterations with the closed loop combination of the guidance and dynamics simulations. The result is a closed loop nominal trajectory.

In this analysis the sequence was varied somewhat in that the simulations were constructed and checked out in this manner but almost all of the guidance constant and launch date, time and azimuth were changed to agree with GD/C constants provided in Reference 1. The result is a minor mismatch of simulation and dynamics since the GD/C constants were obtained using a quite different simulation model.

3.3 Disturbance and Dispersions

The final and most important phase of the analysis was to determine the capability of the guidance equations to maintain an acceptable impact when the trajectory is affected by various changes to the vehicle and atmospheric models. A list of anticipated 3σ disturbances was compiled from References 1 and 2 (see Section 7).

The guided flight simulation is subjected separately to each of the disturbances. The resulting dispersion in the injection conditions and impact are the desired results. The dispersions were studied to determine the most troublesome and the possible improvements in guidance equations and targeting which might be made to provide better control in the presence of disturbances.

4. APPROXIMATIONS IN THE STUDY

The approximations and modifications in the various simulations were made on the basis that the real world can be represented with sufficient accuracy without developing more precise models. This section of our performance analysis discusses these modifications and approximations.

4.1 Vehicle Model Approximations

The simulation model of the vehicle contains many implicit approximations. Prior experience has shown that none of these approximations seriously degrade the accuracy of the simulation while they do save computer memory and simplify the program. For instance, the Centaur engine model is simulated as a simple fixed thrust, fixed weight flow device. Although an elaborate engine model exists for the Centaur engines, it has been found that it adds little to the significance of the simulation but requires considerable additional memory capacity. Similar statements apply to the thrust build-up and decay impulses, the control jets and lubrication oil mass flows and the general tabular entries for center-of-gravity, center-of-pressure locations, tanking pressures, etc.

4.2 Trajectory Approximations

In this analysis the nominal trajectory is what occurred when GD/C's constants and equations were used in the simulation. Since the resultant trajectory had a 90 n. mi. parking orbit, a true anomaly of about 4 degrees at injection, a satisfactory burn-out-weight and impacted at a reasonable spot on the moon, no attempt was made to refine the trajectory.

4.3 Guidance Equation Approximations

Several approximations and modifications were made in the guidance and control system simulations. These changes and the reasons for them are discussed below.

4.3.1 Control System

The simulation of the control system requires consideration of the rotational dynamics of the vehicle as well as the translational dynamics normally simulated. The accurate numerical integration of the rotational equations of motion requires a significantly shorter integration step size than the translational motion integration required because of the dynamical ranges involved. Thus, the computational step size for the entire simulation must be decreased significantly when the full control system

simulation is used. Since running time on the IBM 7094 would be increased by over a factor of 10 if the Atlas/Centaur control system were simulated and since many cases must be simulated for a detailed performance analysis, it is not economically feasible to use the control system simulation except for special cases. For this reason a compromise simulation was used which provided a steering signal proportional to the steering error without requiring excessive memory space or reduction in cycle time.

4.3.2 Computation Step Size

The cycle time required by the actual flight computer depends on the number of computations required per cycle. This varies for different phases of the flight. In this simulation a 1 sec cycle time was adopted for the booster and sustainer stages, 1.25 sec for both Centaur burns and 2.0 sec for parking orbit. These cycle times should be small enough to give realistic truncation errors.

4.3.3 Sigmator Simulation

In the flight computer a special section called the sigmator is used both to accumulate the measured velocity pulses from the accelerometers and to perform real-time rectangular integration of these pulses to obtain the corresponding position. Rather than simulate such a system, the dynamics simulation was programmed to provide equivalent outputs to the guidance at each cycle of computation by using the velocity and position resulting from all nongravitational accelerations. These positions and velocity data are more accurate than the sigmator data would be.

4.3.4 Inertial Measurement Unit (IMU) Simulation

In the actual guidance system, the inertial instrument outputs must be corrected for instrument scale factor, bias and nonlinearity by a set of 'd' coefficients. In this simulation, however, the instrument output (from the dynamics simulation) is accepted as ideal with unity scale factor and no bias or nonlinearities. This permits program simplification and detracts nothing from evaluation of the guidance equations.

4.3.5 Deviations from GD/C Guidance Equations

The Two-Burn GD/C guidance equations given in Reference 1 and updated in reference 3 were not programmed exactly for this simulation. The major change is that the phase branching was altered to permit the use of previous TRW programming. Functionally the program is similar but the switching logic varies.

4.3.5.1 Initial Computations

All launch-on-time polynomials were simulated exactly. Many initialization constants were not required because the initial values for iterative square roots were not

needed.

4.3.5.2 Navigation Computations

The basic navigation equations were simulated exactly. However, because a sigma-tor was not simulated a method had to be devised to zero the sigma-tor output during parking orbit and effectively reinitialized at the beginning of second burn. To accomplish this four branches were provided. The first is used throughout first burn and transmits the dynamics sensed velocity and position to the guidance. The second zeros these guidance inputs during parking orbit. The third is used for one cycle only, to record the initial value of sensed velocity and position for second burn. The last branch converts the dynamics output to give the effect of having rezeroed the sigma-tor at the beginning of second burn.

4.3.5.3 Coordinate System and Phase Branch

The coordinate system equations used are the same as those used by GD/C but the yaw steering computations are included at this point rather than later. Functionally this does not affect the simulation. The phase branches are changed significantly from those shown by GD/C in their latest charts but the sequence of calculations is not affected. A different branching was used in this simulation only to avoid changing the basic structure of an earlier simulation which was used in constructing this one.

4.3.5.4 Booster Phase

The booster program is functionally identical to that of GD/C.

4.3.5.5 Sustainer Phase

The organization of the flow diagrams for the sustainer phase guidance is considerably different than that of GD/C but with the exception of the lack of a back-up SECO discrete it is functionally the same.

4.3.5.6 Centaur First Burn Phase

The Centaur first burn guidance equations are functionally the same as those of GD/C with the exception of the cut-off routine count-down loop. In this simulation the MECO discrete is issued by checking the flight time against the desired cut-off time with successively smaller time steps.

4.3.5.7 Parking Orbit

Except for branching techniques and telemetry all of the GD/C functions for the parking orbit are performed by this simulation.

4.3.5.8 Centaur Second Burn

The second burn Centaur program is functionally the same as that of GD/C.

4.3.5.9 Post Injection Phase

The post injection simulation is the same as GD/C's except that no steering is permitted. This is done because the simulation is mechanized in such a way that this maneuver would ruin the trajectory of the spacecraft.

4.3.5.10 Cutoff Routine

The two major differences in the cutoff routine are the absence of the sigma-tor countdown loop and the subroutine exit logic. These functions are handled in a different manner in this simulation.

4.3.5.11 Steering Subroutine

There are no functional differences in this subroutine.

5. PERFORMANCE CRITERIA

The basic performance criteria used for analysis of the two-burn equations were the impact miss, payload capability and Figure-of-Merit (FOM). In order to be able to compare data from this analysis to the GD/C results additional criteria for both parking orbit and final injection were adopted.

5.1 Figure-of-Merit

The FOM's used in this report are not true FOM's in the sense of numbers derived from sensitivity coefficients. They are, however, useful in providing a rough over-all measure of the effect of the perturbations. They can be envisioned as coarse estimates of the magnitude of velocity correction required 20 hours after final injection. The relations used are:

$$\text{FOM 1} = R \frac{\sqrt{(\Delta \text{LAT})^2 + (\Delta \text{LONG})^2 \cos^2 \text{lat}}}{\text{TF} - 72,000}$$

$$\text{FOM 2} = \frac{\sqrt{(\Delta \bar{B} \cdot \bar{R})^2 + (\Delta \bar{B} \cdot \bar{T})^2 + (\Delta T \text{ VEL}_\infty)^2}}{\text{TF} - 72,000}$$

Where R = Selenographic Radius at impact in meters
 ΔLAT = Error in selenographic latitude in radians
 ΔLONG = Error in selenographic longitude in radians
 Cos LAT = Cosine of nominal selenographic latitude

TF = Time from final injection to impact in seconds

$\Delta \bar{B} \cdot \bar{R}$ = Error in $\bar{B} \cdot \bar{R}$ direction in meters

$\Delta \bar{B} \cdot \bar{T}$ = Error in $\bar{B} \cdot \bar{T}$ direction in meters

ΔT = Error in arrival time in seconds

VEL_{∞} = Hyperbolic impact velocity in meters per second.

When comparing to the GD/C results in Reference 1 the relation given in their report was used.

$$MCS = \frac{\sqrt{(\Delta \bar{B} \cdot \bar{R})^2 + (\Delta \bar{B} \cdot \bar{T})^2}}{TF - 72,000}$$

5.2 Impact Criteria

Four parameters were used as criteria for the impact errors. The physical miss of the target is shown in terms of selenographic latitude and longitude errors. The selenographic coordinate system being referenced so that zero degrees latitude is at the lunar equator and zero degrees longitude is on the mean earth moon line (Sinus Medii). Two other parameters used to judge the impact control are the time-of-arrival and the impact velocity. The time-of-arrival dispersion is the difference in the Greenwich mean time and not of time in free flight.

5.3 Final Injection Criteria

The primary criteria used at final injection is the dispersion in the Centaur burn-out weight. This parameter measures the payload capability control.

The perigee, altitude, circular range and vis-viva energy dispersions are all measured in terms of actual vehicle dispersions and not guidance measured values.

The references for altitude measurements is an analytic sea level radius based on latitude and ellipticity. The reference for perigee is the mean radius of the referenced geoid. The combination of the altitude and circular range dispersions allow a measurement of the ability of the guidance equations to control the location of final injection. This also established their ability to keep the final injection centered in the "injection box" for which the required velocity polynomials are designed.

5.4 Parking Orbit Cutoff

An artificial parameter ϕ was devised to show the effect of perturbations on the parking orbit without the sampling effects of the computer cycle time. The parameter ϕ is an angle which exists between the radial position vector at cutoff and the nominal radial position vector if the computer operated on a continuous rather than sampled time basis. The angle is given in 10^5 radians. To obtain a feel for magnitude significance, a ϕ of 238 is equivalent to 2 sec of coast time or 7.786 n. mi. of circular range. It is important to remember that because of the computer sampling, the cutoff is more accurate than this data might indicate and also the more often the sampling occurs the more accurate the cutoff will be.

5.5 Parking Orbit Injection

Two parameters were used as criteria for parking orbit injection. The first is the aerodynamic heat acquired during the ascent through the atmosphere. It is obtained from the expression,

$$H_A = \int Q V_a dt$$

where

Q is the dynamic pressure

V_a is the airspeed.

The dispersions in H_A should be a reasonably good indication of how well the pitch profile is controlled.

The second parameter is the parking orbit perigee. A minimum perigee altitude of 86.5 n. mi. has been established as the point at which drag will become excessive. The dispersions given are true vehicle perigee dispersions not guidance values.

6. GUIDANCE CONSTANTS

An attempt was made in this analysis to use all of the guidance constants given by GD/C in their Two-Burn report (Reference 1). However, seven constants were changed, five added and 13 not used (see Table 6.1).

All of the initial guess constants (I7, I8, I9, I10, K20, K23) and the two iteration controls (I12, E17) were not required because the simulation used the IBM 7094 square root algorithm. All of the remaining constant changes were required to update the guidance equations in accordance with Reference 3.

Table 6.1
Guidance Constants

GD/C	TRW	Title	GD/C Value	TRW Value
I7	-	Initial guess for a_T	4.5	N.A.
I8	-	Initial guess for Y	20,000	N.A.
I9	-	Initial guess for V_{rt}	20,000	N.A.
I10	-	Initial guess for f	20,000	N.A.
I12	-	Number of f iterations	2.0	N.A.
E5	-	Sustainer integral steering	25.0	N.A.
E7	-	Centaur one integral steering	31.0	N.A.
E12	-	Centaur two integral steering	55.0	N.A.
E17	-	PIJ number of f iterations	10.0	N.A.
K20	-	Initial guess for f	15,000	N.A.
K23	-	Initial guess for f	36,000	N.A.
E11	-	Orbit cutoff bias	0.596×10^{-3}	N.A.
J32	-	V_{rr} coefficient for M^2	0.4209331×10^4	N.A.
E6	E8	Guidance SECO Detector	0.1	100.0
E9	E10	Centaur one MECO backup	340	434
E16	E17	PIJ retromaneuver	204	65
K13	K17	Radial Velocity bias	12	8
K18	K12	Yaw steering gain - antipode	0.155×10^{-8}	0.14333×10^{-4}
J25	J38	Nominal R_m polynomial	21,501,444	21,505,343
J26	J38	Nominal R_m polynomial	0.55954468	21,505,343
-	E7	Yaw steering antipode control	-	0.03
-	E12	Integral steering limit	-	0.006
-	E14	100 lb thrust timer	-	120
-	J32	Parking orbit cutoff backup	-	2100
-	J33	Parking orbit cutoff backup	-	0

The reference 3 changed the integral steering technique (E5, E7, E12, new E12), the yaw steering (K18, new E7), the V_{rr} polynomials (J32, J25, J26) and the timing references (E6, E9, E16), added 100 lb thrust phases to the parking orbit (New E16) and modified the parking orbit cutoff (E11, J32, J33).

The radial velocity bias constant K13 was changed somewhat arbitrarily. Apparently with GD/C's simulation models the value of 12 ft/sec gives satisfactory results since they have used it several times. However, in TRW's simulation models this value gives a resultant real world radial velocity of 3 ft/sec instead of zero. Since previous independent guidance constant generations had given more satisfactory results with 8.0 ft/sec, this value was substituted.

The values of several guidance constants were changed for individual perturbations runs in some cases. The 114° launch azimuth 7 December trajectory had a nominal parking orbit time of 94 seconds. This was too short for the standard value of E14 (120 sec) so it was reset to 60 seconds for these runs. The 90° launch azimuth 21 October run had too long a parking orbit (1800 sec) to allow play around the backup cutoff (J32). Therefore for these runs J32 was reset to 2500 seconds. It was also necessary to reset the energy level (E15) for entering second burn cutoff on three of the perturbation runs. The energy apparently changed too rapidly on these runs for the standard GD/C value of 13,000,000 ft²/sec², so for these cases E15 was reset to 14,000,000 ft²/sec².

The liftoff times used in the simulation were obtained by telephone from GD/C. They were:

21 October	90°	40,096.500 sec
	102°	46,967.842 sec
	114°	53,901.622 sec
7 December	90°	23,742.966 sec
	102°	28,401.900 sec
	114°	31,197.018 sec

7. PERTURBATIONS

An attempt was made in this analysis to use the same perturbations as GD/C and apply them in a similar manner. Two different sets of perturbations were used. One reasonably complete set is similar to those used by GD/C for their AC-7 performance analysis (Reference 2). A second set is similar to the abbreviated set used by GD/C in the preliminary AC-8 performance analysis (Reference 1). Since most of these perturbations have been adequately discussed elsewhere (Reference 4), only the parking orbit and composite dispersions will be discussed here.

7.1 Parking Orbit Perturbations

Two perturbations were used for parking orbit. The ullage rocket thrust was perturbed by ± 1 lb and the parking orbit termination was perturbed by ± 2 sec.

The one pound thrust change was selected arbitrarily because it was not believed to be a significant perturbation. Subsequent study has indicated that the actual thrust variation for each engine is about 5%. In addition the atmospheric drag at this altitude should be accounted for and this can vary as much as 0.2 pounds. Based on this data a perturbation value of about 0.24 pounds would seem reasonable for future analysis.

The ± 2 sec parking orbit cutoff perturbation was performed to determine the maximum effect of the computed cycle time increment on the cutoff. The perturbation was applied by changing the two guidance constants (J36 and J37) just enough to cause the cutoff to jump one compute cycle.

7.2 Composite Perturbations

Four composite perturbations were used in this analysis. The first was an Atlas liftoff weight composite. In order to perturb the Atlas liftoff weight correctly in the TRW simulation, some of the mass added is dry weight and some fuel and lox weights. GD/C's simulation apparently automatically apportions a lumped mass into the correct proportions of dry weights and propellants and they therefore do not define the "Atlas liftoff weight $\pm 157^4$ lbs" given in Reference 1 further. In order to have a liftoff weight perturbation for a rough comparison to GD/C the four independent mass perturbations used in the AC-7 performance analysis (Reference 2) were combined into one composite.

Atlas Liftoff Weight

Atlas fuel tanking	+ 875 lb
Atlas lox tanking	+ 1300 lb
Booster Jettison weight	+ 93 lb
Sustainer Jettison weight	+ 285 lb

This perturbation is applied as an increase of 2553 lb in liftoff weight - 285 lb of dry weight, 875 lb fuel and 1300 lb lox. The weight lost at booster jettison is increased by 93 lb. The sustainer jettison weight is carried up to Centaur separation.

The remaining three composite perturbations were used to test the sensitivity of the guidance equations across the launch window. The high and low composites are direct opposites and are composed of the following independent perturbations:

	<u>High Composite</u>	<u>Low Composite</u>
Booster Pitch Program	- 5%	+ 5%
Booster Thrust	+ 3000 lb	- 3000 lb
Sustainer Thrust	+ 855 lb	- 855 lb
Sust/Cent Thrust Misalign (Pitch)	+ 424 lb	- 424 lb

The lateral composite perturbation was to the right and was made up of two independent variations

Right Composite

Launch azimuth	+ 2 deg
Sust/Cent Thrust Misalign (Yaw)	- 2 deg

8. RESULTS OF THE PERFORMANCE ANALYSIS

Inserting the perturbations discussed in Section 7 into the closed loop simulation caused a corresponding set of dispersions. These dispersions are tabulated in Tables 8.1, 8.2, 8.3, and 8.4. The data listed in the tables are in agreement with the performance criteria discussed in Section 5. All data shown is for a launch date of 21 October 1964 on a launch azimuth of 102 degrees unless otherwise stated.

8.1 The Complete Performance Analysis

Tables 8.1 and 8.2 list the dispersions caused by a complete set of positive and negative perturbations respectively. The data is grouped into types of perturbations (i.e. propulsion, mass, etc.) and the various times in the flight. The root-sum-square, rss, for each of the groups and the total number of dispersions is given. For an overall effect of both positive and negative perturbations, the corresponding dispersion rss's can be averaged. The parking orbit dispersions were not included in the overall rss because the magnitude of the perturbation has not yet been agreed to with GD/C.

8.1.1 Atmospheric Heating Dispersions

The perturbations which caused the most significant heating dispersions were predictably the Booster Pitch Program and the Atmospheric Density. The nominal heating limit is 108,000,000 lb/ft and the nominal trajectory heating is 107,636,220 lb/ft. The 3 σ heating limit is 128,000,000 lb/ft which is just slightly more than sum of the nominal heating and the average rss dispersion magnitude 127,976,220 lb/ft. Thus the trajectory design is just within the heating limits. The guidance equations and constants actually have little to do with the heating since on the nominal flight the accumulated heat is already 106,145,203 lb/ft prior to admitting guidance steering.

8.1.2 Parking Orbit Perigee

The first burn altitude control function provides excellent control of both the parking orbit injection altitude and perigee. Although only the perigee dispersions are given, the altitude dispersion differed by only tens of feet. The three largest dispersions were caused by the Centaur thrust, Centaur weight and Hold Down Time. The Hold Down Time dispersion is probably caused by the flight time dependence of the altitude control function. The difference in the perigee rss and the altitude rss was 61 ft.

8.1.3 Parking Orbit Cutoff

The dispersions of the parameter ϕ indicate the relative effect of the perturbations on the cutoff independent of the computer sampling interval. With the 2 sec sampling time used in parking orbit the cutoff was quite accurate in most cases. With

a shorter sampling time corresponding improvements can be expected. The influence of the perturbation however, remains fixed. The five most significant perturbations are in order; the Hold-Down Time, the Tailwind, the BECO Discrete, the Booster Pitch Program, and the Centaur weight. The accuracy of the cutoff is primarily affected by time, velocity and range errors at injection into the parking orbit. Figure 8.1 is a plot of range angle versus time showing the cutoff points for three perturbed runs and the nominal run. Note that the BECO perturbation even though it has a large influence on the cutoff, cuts off at almost the same range angle as the nominal run. On the other hand the Lox Tanking perturbation while not having as much influence, cuts off at a significant distance from the nominal cutoff (but exactly on the desired cutoff). Results of this type indicate that the simulation should use a precise parking orbit cutoff and account for imprecision in the cutoff by adding an additional perturbation equivalent to one sample time.

8.1.4 Final Injection Altitude and Perigee

The most interesting feature of the dispersions for final injection altitude and perigee is that the perigee dispersions are much smaller than the altitude dispersions. Both dispersions are small compared to the Direct Ascent method (Reference 2). The only significant dispersion which might be unexpected was the Hold-Down Time. This is apparently a secondary effect of the dispersions in parking orbit cutoff.

8.1.5 Final Injection Range

The dispersions of the circular range at cutoff are primarily dependent on the precision of the parking orbit cutoff. This is natural since the duration of the second burn is essentially fixed by the energy cutoff. Thus perturbations which cause large parking orbit cutoff dispersions may cause large range errors. However, because of the sampled nature of the parking orbit cutoff this was not necessarily true. Here also a decrease in the sampling interval on the parking orbit cutoff will improve the range dispersions. Since the altitude dispersions are small, an improvement in the range dispersions will reduce the variations in the radial required velocity giving more uniform results.

8.1.6 Final Injection Vis-Viva Energy

The injection energy dispersions shown are the true vehicle energy dispersions.

For this trajectory it can be seen that the impact errors and FOM are strongly correlated to this parameter. However, the true energy dispersions can only be partially controlled. The guidance equations attempt to cutoff the engines when the guidance energy has reached a desired value. The present equations do this well, the worst dispersion in cutoff being $4200 \text{ ft}^2/\text{sec}^2$. The other contributor to vehicle energy dispersions is the dispersion in the navigation error and this is uncontrolled. The magnitude of the dispersions (normally 100 ft and 0.1 ft/sec) make it unlikely that it will be controlled. Of particular importance is the navigation error dispersion caused by the guidance equation lock-out of the parking orbit thrust accelerations. The basic 4 lb. thrust effect is accounted for in targeting but as the 1 lb. perturbation shows, changes to the thrust level result in large navigation error dispersions and large injection energy dispersions. For information purposes a plot of the navigation errors for the nominal trajectory is given in Figure 8.2.

8.1.7 Final Injection Vehicle Weight

As a class the negative dispersions are worse than the positive dispersions. This is primarily due to the larger dispersions for negative Booster Pitch Program and Tailwind perturbations than for the Headwind and Positive Booster Pitch Program perturbation. It should be noted however, that the Booster Pitch Program perturbation detracts from the payload capability in both directions. The overall weight dispersion rss's are competitive with those reported by GD/C for the AC-7 Direct Ascent (Reference 2). As for AC-7, the ISP and Tailwind perturbations have the most significant dispersions.

8.1.8 Impact Time of Arrival

The dispersions in the impact time are directly correlated to the dispersions in true injection energy (see Figure 8.2). Minor deviations from this relation can be traced to changes in the trajectory orientation.

It is significant that the rss of the dispersions is about three times worse than those given for AC-7 (Reference 2). Since both sets of guidance equations use the same cutoff technique the difference is probably due to navigation errors. This would be reasonable in view of the short guided flight time of the direct ascent mission (680 sec) compared to that for this flight (2135 sec).

8.1.9 Impact Velocity

The impact velocity dispersions are also strongly correlated to the injection energy dispersions (see Figure 8.4). Lack of exact correlation is again attributed to orbit orientation changes.

8.1.10 Impact Miss

The impact latitude and longitude dispersions are largely caused by dispersions in the injection energy and in orbit reorientations caused by azimuth perturbations. Figure 8.5 shows that most of the longitude dispersions are tightly correlated while the latitude dispersions are quite loose, some being far off the correlation line. This is explainable in terms of the impact plot (Figure 8.6) which shows that the longitude error is mostly the miss magnitude while the latitude error is more susceptible to trajectory orientation changes. The impact plot shows that most of the dispersions fall along the intersection of the trajectory plane and the lunar surface. The three major exceptions are the Launch Azimuth, Thrust Misalignment in Yaw, and Crosswind dispersions which have large effects on the orbit orientation. Generally dispersions with high injection energies arrive early and impact ahead (East) of the target, while low energy dispersion impact behind the target.

8.1.11 Figure-of-Merit

The FOM's for this Two-Burn trajectory are three to four times larger than those for the AC-7 Direct Ascent trajectory discussed in Reference 2. This does not seem to be caused by sensitivity to particular perturbations as much as the result of random effects from second burn cutoff errors and navigation error dispersions. Figures 8.7 and 8.8 show the strong dependence of FOM on the injection energy dispersions. As noted previously the dispersions from azimuth perturbations do not fit the general energy dependence pattern because of orbit orientation changes.

Of particular interest are the FOM's caused by the parking orbit thrust perturbations. Tables 8.1 and 8.2 show that miss-plus-time FOM's of 9 m/s can be expected with a 25% perturbation in the parking orbit thrust. Recent estimates of the dispersions using more accurate perturbations indicate that these FOM's will be closer to 2 m/s. This means that this will be the most significant software perturbation. Current GD/C computations of the miss-plus-time FOM which would be encountered if the type 177 accelerometers were allowed to sense the thrust acceleration are about 5 m/s for this length of coast.

8.2 Comparison of Results to GD/C Performance Analysis

In Reference 1, GD/C reports on a performance analysis with selected perturbations for the 21 October 1964 and 7 December 1964 launch dates. In order to cross check the TRW simulation performance using the GD/C constants, the GD/C analysis for the 102 degree launch azimuth on 21 October 1964 was repeated. Table 8.3 gives a comparative list of both GD/C and TRW results. The comparison is generally quite good except for the MCR's.

The disagreement in MCR's between TRW and GD/C is not unusual since this parameter is most sensitive to differences in the simulations. GD/C and TRW undoubtedly have minor differences in the vehicle models and dynamics simulations. The sustainer I_{sp} dispersions are probably a good example of this since they are heavily dependent on the vehicle weight, propellant tanking, and SECO criteria. The Atlas lift-off weight dispersions are caused by the different methods of applying the perturbation as discussed in Section 7. The major point to remember here is not that TRW is trying to obtain identical results to GD/C but that we are trying to establish whether the TRW simulation exhibits similar guidance equation control of the dispersions. The fact that Table 8.3 does show equivalent control even though there are differences in the two simulations should give more confidence in the two performance analysis.

One problem that did raise some doubts was yaw steering control. TRW obtained the latest configuration of yaw steering by using the equations from the latest flow diagrams (Reference 3) and modifying the GD/C constants from Reference 1 to fit. This most likely resulted in the incorrect yaw gain. The equation performance was correct in that it nulled the $\dot{\epsilon}_y$ parameter but the dispersions caused by azimuth perturbations indicated that this may not be enough. Table 8.4 shows the GD/C and TRW dispersion resulting from application of launch azimuth perturbations to three different launch azimuths for 21 October 1964. Notice that the altitude and weight dispersion agree very well but the MCR's are significantly different. This would seem to say that the method used in Reference 3 is not as good as that used in Reference 1 or that TRW's yaw gains are not good enough. In any case the dispersions in V_{mn} (essentially out of plane velocity) are significant at injection (± 55 ft/sec).

The yaw gain switch near the antipode was not a smooth transition. Although the gains were calculated to complement each other, the transition is affected by a change

in the value of ϵ near the antipode. As a result there are some significant yaw transients at the start of the second burn.

8.3 Launch Window Study

A very brief check was made of the launch-on-time polynomials for both the 21 October 1964 and 7 December 1964 launch dates. This was accomplished for launch azimuths of 90, 102 and 114 degrees on both launch dates using the launch times given in Section 6. Figure 8.9 is a plot of the six lunar impacts. The large dispersion in the 21 October 1964 launch data was later found to be caused by a guidance constant change by GD/C after targeting was completed. The 7 December 1964 launch date gave much better results. Table 8.5 shows the dispersion data for both launch dates. All dispersions are referenced to the nominal parameter values for the launch date and azimuth considered. Of particular interest is the large payload dispersion caused by the Low Composite perturbation. This result could not have been predicted by combining the individual dispersions included in the Low Composite. The uncomfortable conclusion drawn from this is that the rss summary is not necessarily a good indication of possible worst case problems. No impact data is shown for two of the 7 December 1964 Low Composite runs because a simulation problem in these runs caused a poor cutoff at final injection.

Table 8.1
Complete Non-Nominal Performance Analysis - Positive Dispersions Trajectory
21 October 1964 Launch Azimuth 102°

	P.O. Injection	Cut-Off	Final Injection					Impact			FOM			
	Value	(H.P. 10 ⁵ lb/ft. (rad)	Perigee (ft)	Alt (ft)	Perigee (ft)	Range (ft)	Energy (ft/sec) ²	Wt (lb)	Arr. Time (sec)	Imp. Vel. (m/s)	Lat. (deg)	Long. (deg)	Miss Only (m/s)	Miss + Time (m/s)
Perturbation														
Booster Thrust	+3000 lb	-2763	-3036	-583	+663	-29187	+6117	+14.7	-30.6	+115	-054	-472	.098	.273
Sustainer Thrust	+855 lb	-814	+121	-1217	-49	-27040	+5792	+8.2	-28.6	+108	-053	-450	.094	.256
Centaur Thrust	+424 lb	-	+4695	-3569	-1121	-58185	+1408	+7.2	-0.8	-003	-010	-006	.002	.019
Booster ISP	+2.4 sec	+119	+859	-745	-336	-8499	-2912	+47.0	+19.0	-066	+040	+222	.047	.167
Sustainer ISP	+2.8 sec	+35	+224	+660	-110	+18652	-8511	+29.4	+46.4	-150	+085	+656	.137	.409
Centaur ISP	+3.6 sec	-	-806	+1273	+123	-27278	-5984	+92.0	+32.0	-105	+066	+406	.085	.268
RSS														
Lox Tanking	+1300 lb	-2883	5720	4144	1356	78312	13772	111.0	72.6	.251	.138	1.034	.216	.638
Fuel Tanking	+875 lb	+1692	+1572	-663	-417	-6350	+160	+5.6	-0.2	+002	-005	-002	.001	.004
Booster Jet Wt	+93 lb	+1085	+1220	+5	-339	-8264	-5072	+20.0	+28.1	-094	+052	+393	.082	.246
Sust Jet Wt	+285 lb	+1202	+184	-124	-20	-2522	+1445	-5.2	-8.4	+030	-017	-113	.024	.074
Centaur Wt	+422 lb	+544	-3884	-772	+17	-19404	+7326	-27.5	-40.2	+160	-080	-566	.118	.357
RSS														
Booster Pitch Program	+5%	-2332	1369	1026	956	-29306	9518	45.4	59.2	-070	+053	+279	.059	.179
Sust/Cent Thrust Miss (Pitch)	+2 deg	+18545	-1399	-1048	+198	-28593	+6000	-23.4	-31.6	+116	-034	-448	.093	.269
Centaur Thrust Miss (Yaw)	+2 deg	+1	-381	-491	-510	+786	+4912	-2.0	-27.4	+102	-025	-452	.094	.249
Centaur Rate Gyro Drift (Pitch)	+0.1 deg	-	-22	-46	-53	+100	+816	-0.0	-4.4	+017	-009	-076	.016	.044
Centaur Initial Att (Yaw)	+0.1 deg	-	0	-8	-8	+9	+224	0	-1.3	+005	-002	-019	.003	.010
Centaur Initial Att (Pitch)	+10 deg	-	-685	+189	+144	+1147	+144	-0.8	-1.5	+006	-006	-022	.005	.015
RSS														
Drag Coef & Norm Force	+5%	-18545	1607	1175	-580	-28640	7838	23.6	42.4	.178	.170	.644	.138	.377
Atmospheric Density	GDC	+130	+352	-748	-100	-16041	+4469	-11.8	-23.9	+092	-048	-334	.098	.211
Atmospheric Pressure	Tables	+1237	+463	-1265	-167	-27405	+7376	-20.2	-38.6	+153	-062	-544	.113	.342
Atmospheric Temp		-115	+57	-708	-144	-14029	+4000	-10.5	-21.2	+081	-041	-301	.063	.188
Headwind		+2459	-862	-105	-7	-2465	+1328	-4.0	-7.6	+028	-018	-107	.022	.067
Left Crosswind		+237	+142	-149	-127	-384	+9680	-24.7	-50.9	+2208	-085	-712	.148	.450
RSS														
Hold Down Time	+3 sec	13810	1161	2108	313	50783	13660	35.8	71.9	.287	.185	1.011	.209	.639
RECO	+0.06g	-40	+6060	-3153	-1522	-43931	+7440	-1.1	-37.3	+151	-049	-516	.089	.273
Launch Az	+2 deg	+22	+51	-328	-172	-3489	+1840	-2.0	-9.5	+066	+009	+261	.054	.169
RSS														
Total RSS			6096	3196	1558	66171	8324	3.3	40.5	.285	.285	.593	.123	.346
Parking Orbit Thrust	+1 lb	-	9638	5854	2370	121526	20445	127.4	131.9	.500	.419	1.850	.386	1.141
Parking Orbit Cutoff	+2 sec	-	-	+2467	+2773	-12280	+170848	-27.2	-981.2	+2.072	-2.165	-13.226	2.794	8.714
			-	-238	-38	+41044	-3472	-0.2	+13.6	-044	+024	+186	.039	.108

Table 8.2
Complete Non-Nominal Performance Analysis - Negative Dispersions Trajectory
21 October 1964 Launch Azimuth 102°

		P.O. Injection			Out-Off	Final Injection					Impact			POM	
		Perigee (ft)	H.P. (1000 lb/ft)	ω (rad)	Alt (ft)	Perigee (ft)	Range (ft)	Energy (ft/sec ²)	Wt (lb)	Arr. Time (sec)	Imp. Vel. (m/s)	Lat. (deg)	Long. (deg)	Miss Only (m/s)	Miss + Time (m/s)
Perturbation	Value														
Booster Thrust	-3000 lb	+2922	+3021	-60	-1441	-659	-19,468	+5173	-15.7	-27.5	+1.07	-0.50	-383	.080	.244
	-855 lb	-97	+833	-81	-904	-93	-20,319	+4592	-8.1	-23.8	+0.92	-0.35	-334	.070	.212
	Centaur Thrust	-5005	-	-125	+1654	+1121	+11,591	+398	-7.6	-3.1	+0.14	+0.03	-0.068	.014	.042
	Booster ISP	-847	-114	-86	-1334	+215	-38,558	+5392	-46.8	-27.3	+1.03	-0.57	-344	.072	.231
	Sustainer ISP	-188	-33	-28	-676	+91	-18,864	+7541	-29.4	-41.2	+1.64	-0.60	-582	.122	.366
Centaur ISP	-3.6 sec	+810	-	+20	-1278	-144	-27,374	+5968	-92.2	-31.8	+1.21	-0.63	-424	.089	.273
Lox Tanking	-1300 lb	+5917	+3136	+185	+3082	+1332	+59,314	+13,021	+109.2	+69.2	+2.69	-1.31	-949	.198	.607
	-875 lb	-1524	-1659	+42	-1556	+280	-43,803	+4736	-11.4	-21.2	+0.76	-0.41	-306	.064	.180
	Booster Jet Wt	-1110	-1062	-3	-380	+219	-14,613	+7328	-31.5	-40.8	+1.62	-0.75	-578	.121	.363
	Booster Jet Wt	-175	-1192	+1	+128	+12	+2815	-1120	+5.7	-14.9	-0.04	+0.04	+0.079	.016	.050
	Sust Jet Wt	-62	-358	+36	-1206	-40	-27,469	+3152	+27.9	-13.5	+0.49	-0.21	-234	.049	.123
Centaur Wt	-422 lb	+3822	+530	+153	-2042	-796	-28,429	+5952	-29.3	-31.7	+1.17	-0.72	-427	.090	.266
Booster Pitch Program	-5 deg	+3570	-12998	-251	+123	+816	-19,451	+4309	-33.8	-23.3	+0.93	-0.72	-280	.080	.209
	-2 deg	+336	-10	-6	+444	+486	-1258	-4929	+0.3	-26.0	-0.92	+0.28	+451	.094	.248
	-2 deg	+108	-1	-2	-52	-24	-725	-800	+0.8	-6.0	+0.13	+0.154	-0.050	.034	.072
	-0.1 deg	+22	-	0	+30	+30	-83	-96	0	+0.0	-0.01	-0.04	+0.012	.003	.002
	-0.1 deg	0	-	0	-5	-5	+7	+288	0	-1.7	+0.06	-0.08	-0.025	.005	.013
Cent Initial Att (P)	-10 deg	+616	-	-11	-256	-156	-2468	+672	-0.6	-3.7	+0.04	-0.09	-0.053	.011	.034
	-10 deg	-5	-	-2	-35	-8	-678	+336	-0.7	-2.1	+0.08	-0.13	-0.034	.008	.022
Drag Coef & Norm Force	-5 deg	+3612	-12998	-251	+332	+963	-19672	+6845	-33.8	-23.3	+0.93	-0.72	-280	.080	.209
	-2 deg	+336	-10	-6	+444	+486	-1258	-4929	+0.3	-26.0	-0.92	+0.28	+451	.094	.248
	-2 deg	+108	-1	-2	-52	-24	-725	-800	+0.8	-6.0	+0.13	+0.154	-0.050	.034	.072
	-0.1 deg	+22	-	0	+30	+30	-83	-96	0	+0.0	-0.01	-0.04	+0.012	.003	.002
	-0.1 deg	0	-	0	-5	-5	+7	+288	0	-1.7	+0.06	-0.08	-0.025	.005	.013
Atmospheric Pressure	-5 deg	+3612	-12998	-251	+332	+963	-19672	+6845	-33.8	-23.3	+0.93	-0.72	-280	.080	.209
	-2 deg	+336	-10	-6	+444	+486	-1258	-4929	+0.3	-26.0	-0.92	+0.28	+451	.094	.248
	-2 deg	+108	-1	-2	-52	-24	-725	-800	+0.8	-6.0	+0.13	+0.154	-0.050	.034	.072
	-0.1 deg	+22	-	0	+30	+30	-83	-96	0	+0.0	-0.01	-0.04	+0.012	.003	.002
	-0.1 deg	0	-	0	-5	-5	+7	+288	0	-1.7	+0.06	-0.08	-0.025	.005	.013
Atmospheric Temp	-5 deg	+3612	-12998	-251	+332	+963	-19672	+6845	-33.8	-23.3	+0.93	-0.72	-280	.080	.209
	-2 deg	+336	-10	-6	+444	+486	-1258	-4929	+0.3	-26.0	-0.92	+0.28	+451	.094	.248
	-2 deg	+108	-1	-2	-52	-24	-725	-800	+0.8	-6.0	+0.13	+0.154	-0.050	.034	.072
	-0.1 deg	+22	-	0	+30	+30	-83	-96	0	+0.0	-0.01	-0.04	+0.012	.003	.002
	-0.1 deg	0	-	0	-5	-5	+7	+288	0	-1.7	+0.06	-0.08	-0.025	.005	.013
Tailwind	-5 deg	+3612	-12998	-251	+332	+963	-19672	+6845	-33.8	-23.3	+0.93	-0.72	-280	.080	.209
	-2 deg	+336	-10	-6	+444	+486	-1258	-4929	+0.3	-26.0	-0.92	+0.28	+451	.094	.248
	-2 deg	+108	-1	-2	-52	-24	-725	-800	+0.8	-6.0	+0.13	+0.154	-0.050	.034	.072
	-0.1 deg	+22	-	0	+30	+30	-83	-96	0	+0.0	-0.01	-0.04	+0.012	.003	.002
	-0.1 deg	0	-	0	-5	-5	+7	+288	0	-1.7	+0.06	-0.08	-0.025	.005	.013
Right Crosswind	-5 deg	+3612	-12998	-251	+332	+963	-19672	+6845	-33.8	-23.3	+0.93	-0.72	-280	.080	.209
	-2 deg	+336	-10	-6	+444	+486	-1258	-4929	+0.3	-26.0	-0.92	+0.28	+451	.094	.248
	-2 deg	+108	-1	-2	-52	-24	-725	-800	+0.8	-6.0	+0.13	+0.154	-0.050	.034	.072
	-0.1 deg	+22	-	0	+30	+30	-83	-96	0	+0.0	-0.01	-0.04	+0.012	.003	.002
	-0.1 deg	0	-	0	-5	-5	+7	+288	0	-1.7	+0.06	-0.08	-0.025	.005	.013
Launch As	-5 deg	+3612	-12998	-251	+332	+963	-19672	+6845	-33.8	-23.3	+0.93	-0.72	-280	.080	.209
	-2 deg	+336	-10	-6	+444	+486	-1258	-4929	+0.3	-26.0	-0.92	+0.28	+451	.094	.248
	-2 deg	+108	-1	-2	-52	-24	-725	-800	+0.8	-6.0	+0.13	+0.154	-0.050	.034	.072
	-0.1 deg	+22	-	0	+30	+30	-83	-96	0	+0.0	-0.01	-0.04	+0.012	.003	.002
	-0.1 deg	0	-	0	-5	-5	+7	+288	0	-1.7	+0.06	-0.08	-0.025	.005	.013
Total RSS	-5 deg	+3612	-12998	-251	+332	+963	-19672	+6845	-33.8	-23.3	+0.93	-0.72	-280	.080	.209
	-2 deg	+336	-10	-6	+444	+486	-1258	-4929	+0.3	-26.0	-0.92	+0.28	+451	.094	.248
	-2 deg	+108	-1	-2	-52	-24	-725	-800	+0.8	-6.0	+0.13	+0.154	-0.050	.034	.072
	-0.1 deg	+22	-	0	+30	+30	-83	-96	0	+0.0	-0.01	-0.04	+0.012	.003	.002
	-0.1 deg	0	-	0	-5	-5	+7	+288	0	-1.7	+0.06	-0.08	-0.025	.005	.013
Parking Orbit Thrust	-5 deg	+3612	-12998	-251	+332	+963	-19672	+6845	-33.8	-23.3	+0.93	-0.72	-280	.080	.209
	-2 deg	+336	-10	-6	+444	+486	-1258	-4929	+0.3	-26.0	-0.92	+0.28	+451	.094	.248
	-2 deg	+108	-1	-2	-52	-24	-725	-800	+0.8	-6.0	+0.13	+0.154	-0.050	.034	.072
	-0.1 deg	+22	-	0	+30	+30	-83	-96	0	+0.0	-0.01	-0.04	+0.012	.003	.002
	-0.1 deg	0	-	0	-5	-5	+7	+288	0	-1.7	+0.06	-0.08	-0.025	.005	.013
Parking Orbit Cutoff	-5 deg	+3612	-12998	-251	+332	+963	-19672	+6845	-33.8	-23.3	+0.93	-0.72	-280	.080	.209
	-2 deg	+336	-10	-6	+444	+486	-1258	-4929	+0.3	-26.0	-0.92	+0.28	+451	.094	.248
	-2 deg	+108	-1	-2	-52	-24	-725	-800	+0.8	-6.0	+0.13	+0.154	-0.050	.034	.072
	-0.1 deg	+22	-	0	+30	+30	-83	-96	0	+0.0	-0.01	-0.04	+0.012	.003	.002
	-0.1 deg	0	-	0	-5	-5	+7	+288	0	-1.7	+0.06	-0.08	-0.025	.005	.013

TABLE 8-3 COMPARISON OF GDC/TWU NON-NOMINAL PERFORMANCE EFFECTS
LAUNCH DATE: OCTOBER 21, 1964 LAUNCH AZIMUTH: 102 DEGREES

Perturbation Value	First Memo Δr_m (ft)	Minimum Parking Orbit Altitude (n. m.)	Downrange Injection Δr_m (ft)	Injection Δr_m (ft)	Injection Δ Weight (lbs)	MCR (Meters/Sec)
Booster Pitch Profile +5%	-2035	89,565	-15,723	582	-26.5	.107
	-1437	90,661	-28,593	-1048	-23.4	.138
Booster Thrust +5825 lb.	-5009	89,275	836	1874	25.2	.084
	-5986	89,910	-17,377	519	27.1	.072
Booster I.S.P. +3.61 sec.	1622	89,368	34,501	667	81.2	.315
	1316	91,104	10,633	-81	70.8	.247
Atlas Liftoff Weight +1574 lb.	1920	89,521	1,396	465	19.0	.077
	2637	91,348	-16,709	-1374	-2.12	.059
Booster Staging -0.08 g	-844	89,480	-21,662	-515	1.0	.019
	-1228	90,691	-2,637	140	1.14	.067
Sustainer Thrust +1417	292	89,270	2,242	-884	14.1	.097
	188	90,917	-14,096	-772	13.3	.083
Sustainer I.S.P. +3.12 sec.	474	89,596	-2,150	1026	46.3	.246
	238	90,928	-26,248	-1249	32.8	.052
Centaur Weight +401 sec.	-3396	89,560	14,960	584	28.9	.089
	-3734	90,285	-18,228	57	27.6	.079
Launch Azimuth -2 deg.	-547	89,556	-12,622	326	-11.0	.017
	-579	90,782	-10,147	-124	-10.6	.125
Centaur Thrust (1st burn) +424 lb.	3992	89,439	-3,743	-350	46.0	.072
	4766	91,651	-18,289	-1,877	47.3	.089
Centaur Thrust (2nd burn) +424 lb.	0	89,608	-43,202	-1697	-0.1	.089
	0	90,888	-39,847	-1705	-0.2	.090
Centaur I.S.P. (1st burn) +4.95 sec.	-911	89,469	27,609	1365	70.6	.269
	-1133	90,707	25,794	1220	71.3	.191
Centaur I.S.P. (2nd burn) +4.95 sec.	0	89,608	12,396	500	56.4	.096
	0	90,888	11,216	487	54.4	.077
	8847		71,406	3,489	140.7	.538
GDC RSS	9327		74,532	3,689	148.5	.488
TWU RSS						

† All deltas are dispersed minus nominal values.

†† Root sum square.

Table 8.4

Launch Azimuth Dispersion Effects

Launch Date 21 October 1964

Desired Launch Azimuth (Deg)	Actual Launch Azimuth (Deg)	Analysis by	First MECO ΔR (ft)	Injection Δ Weight (lbs)	MCR Miss Only (m/s)
90	88	GD/C	-249	- 7.8	0.121
		TRW	-293	- 7.3	0.095
90	92	GD/C	-170	- 5.3	0.014
		TRW	-437	- 5.5	0.126
102	100	GD/C	-547	-11.0	0.017
		TRW	-579	-10.6	0.125
102	104	GD/C	+ 97	- 2.0	0.112
		TRW	- 26	- 2.4	0.089
114	112	GD/C	-820	-13.7	0.012
		TRW	-814	-13.1	0.210
114	116	GD/C	+346	+ 0.4	0.022
		TRW	+356	+ 0.4	0.098

Table 3.5
Combined Non-Nominal Performance Effects for
21 October 1964 and 7 December 1964 Launch Dates

Perturbation	Launch Azimuth	First Injection		Final Injection		Impact			FOM			
		Perigee (ft)	Heat (1000 lb/ft.)	Alt. (ft)	Perigee (ft)	Weight (lb)	Arr. Time (sec)	Imp. Vel. (m/s)	Lat (deg)	Long (deg)	Miss Only (m/s)	Miss + Time (m/s)
21 October 1964 High Composite	90°	-3953	-15,358	+3874	+2028	+142.0	-25.7	+206	-.045	-.374	.069	.191
	102°	-4037	-15,378	+532	+506	+142.0	-32.8	+130	-.078	-.516	.070	.198
	114°	-4405	-15,439	-949	-1088	+144.1	-18.9	+130	-.071	-.349	.054	.143
Low Composite	90°	-2918	+24,502	+1673	+2362	-220.7	+13.6	-157	+0.16	+404	.070	.147
	102°	-2609	+24,543	-1618	+1052	-221.0	-47.3	+194	-.082	-.624	.084	.268
	114°	-1981	+24,658	-2868	+131	-221.7	-55.6	+399	-.263	-.859	.194	.404
Right Composite	90°	-405	+0	-146	+93	-5.1	-16.7	+0.053	+.461	-.277	.093	.187
	102°	+4	+22	-343	-162	-2.0	-7.3	-.011	-.486	-.553	.066	.117
	114°	+377	+40	-151	-36	+0.9	-6.7	-.173	+.486	-.066	.084	.146
7 December 1964 High Composite	90°	-3955	-15,356	-3540	-3490	+143.58	-9.6	+0.036	-.033	-.036	.009	0.076
	102°	-4104	-15,378	-4310	-4188	+143.79	+1.3	-0.003	-.005	+.067	.013	0.023
	114°	-4519	-15,438	-4880	-4804	+144.9	+3.6	-0.046	-.004	+0.102	.019	0.041
Low Composite	90°	-2919	+24,502	-2684	-1976	-221.0	-	-	-	-	-	-
	102°	-2648	+24,543	-2914	-2124	-221.3	-	-	-	-	-	-
	114°	-2046	+24,558	-2636	-2688	-221.4	+10.3	-0.089	+.113	+.006	.021	.087
Right Composite	90°	-478	+4	-719	-446	-6.3	+14.2	-0.060	-.228	-.008	.043	.132
	102°	-155	+23	-406	-180	-4.2	+26.7	-0.121	-.340	+.093	.068	.236
	114°	+119	+42	-112	+93	-3.1	+38.2	-.711	-.450	+.097	.087	.330

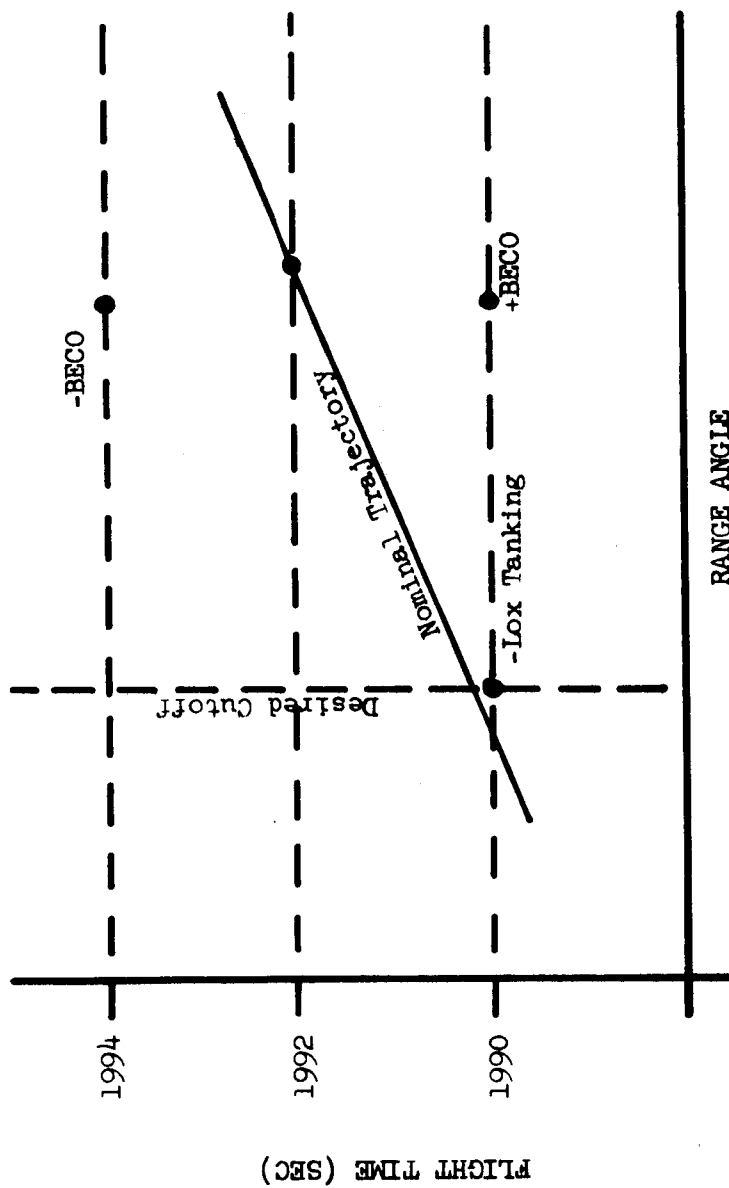


Figure 8.1 - PARKING ORBIT CUTOFF

Launch Date 21 October 1964
Launch Azimuth 102°

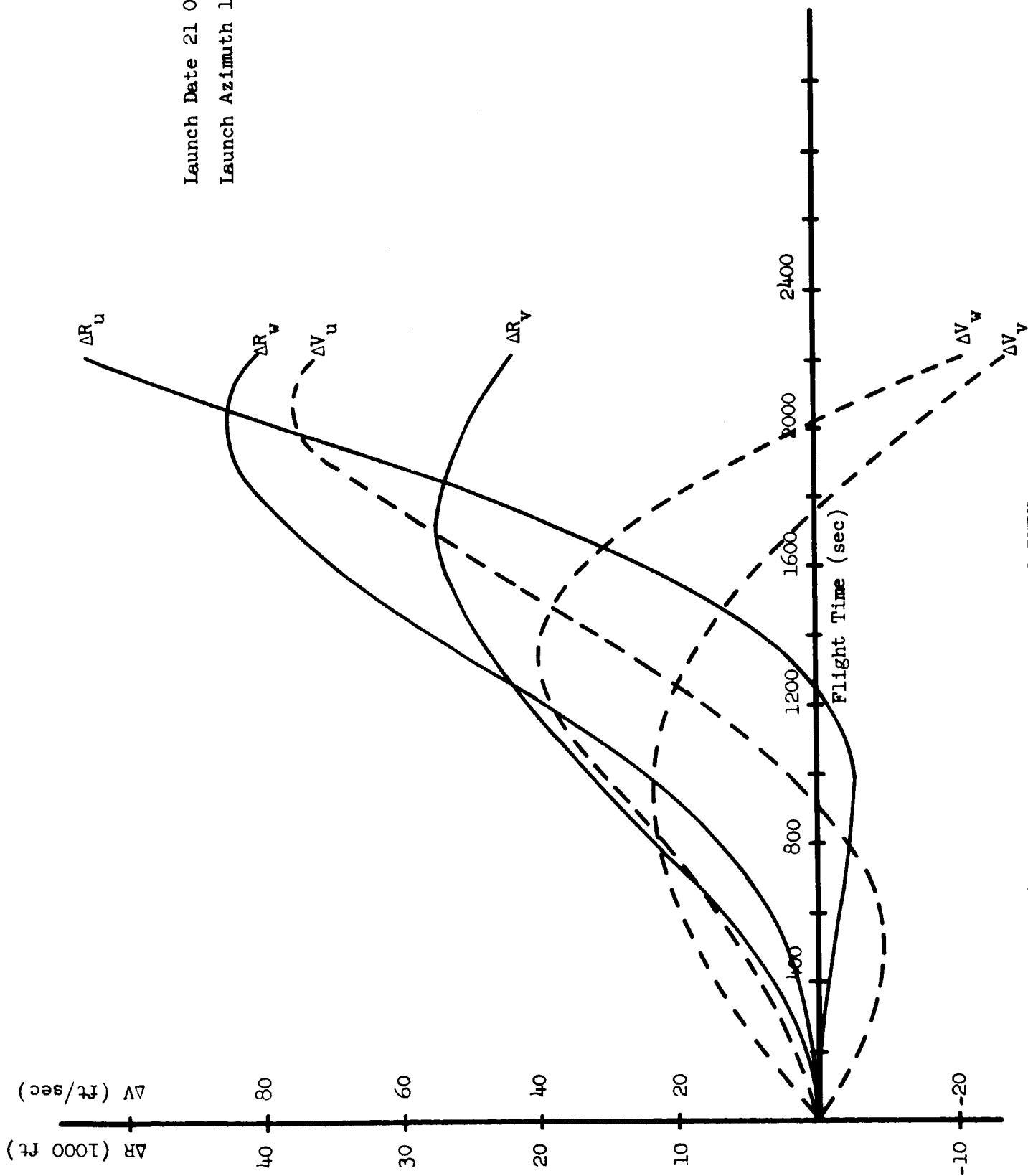


Figure 8.2 - NAVIGATION ERRORS - TWO BURN

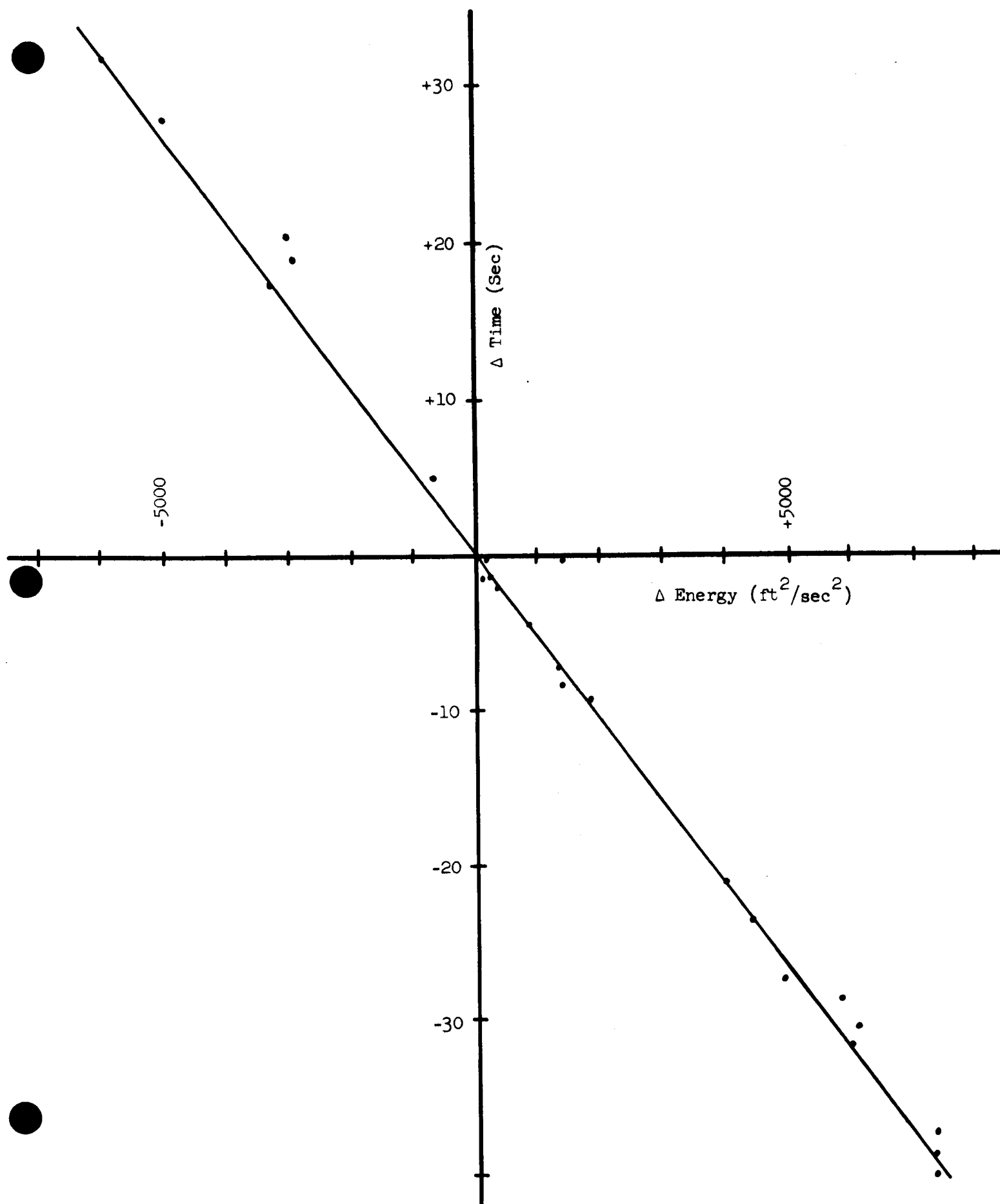


Figure 8.3 - TIME OF ARRIVAL DISPERSIONS vs. INJECTION ENERGY DISPERSION

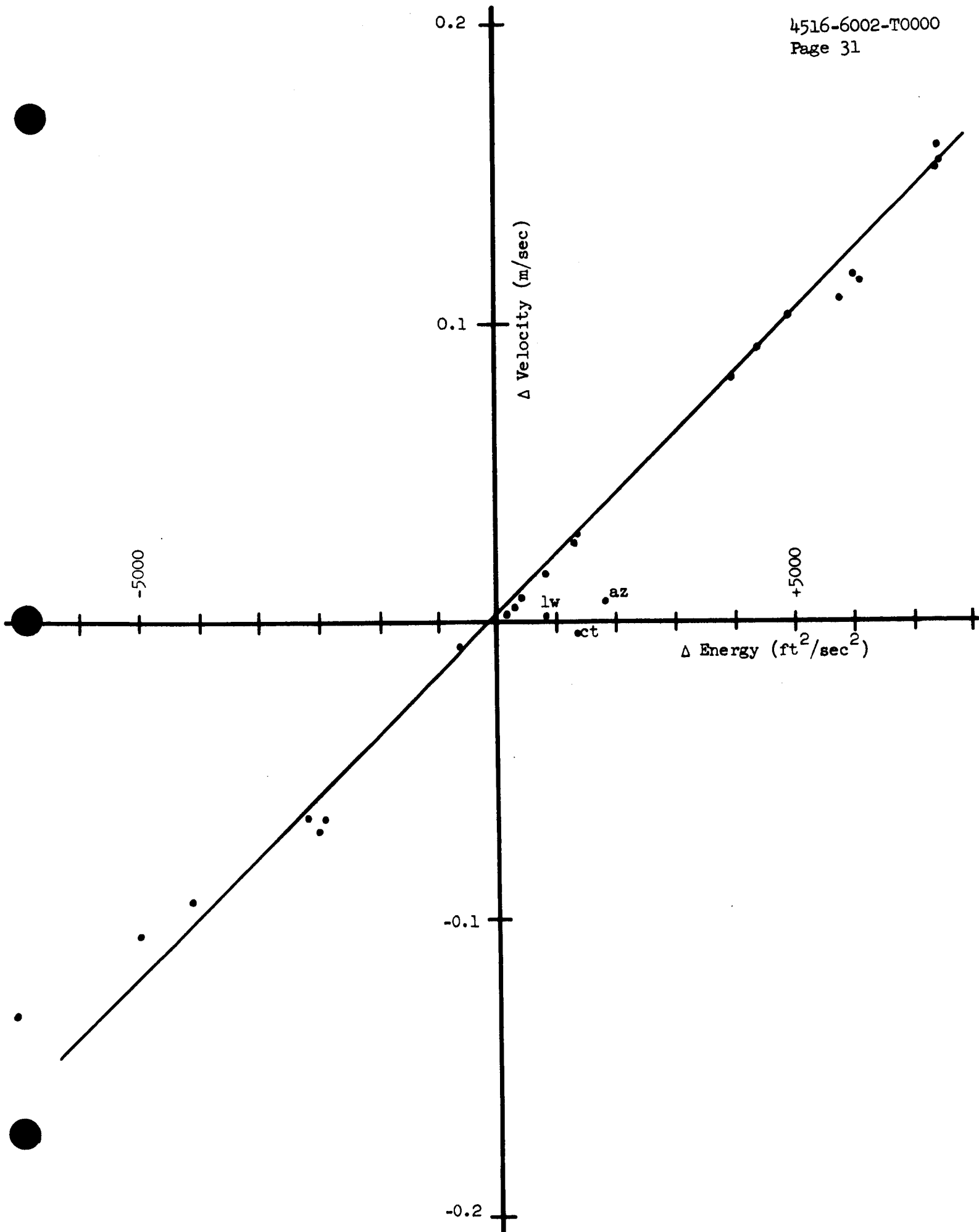


Figure 8.4 - IMPACT VELOCITY DISPERSIONS vs. INJECTION ENERGY DISPERSIONS

+ Latitude Points
• Longitude Points

TMY

+ LCW

0.5 0.1

Δ Longitude (deg)
 Δ Latitude (deg)

-5000

+5000

Δ Energy (ft^2/sec^2)

-0.5 -0.1

-1.0 -0.2

Figure 8.5 - LATITUDE AND LONGITUDE ERRORS vs. INJECTION ENERGY DISPERSIONS

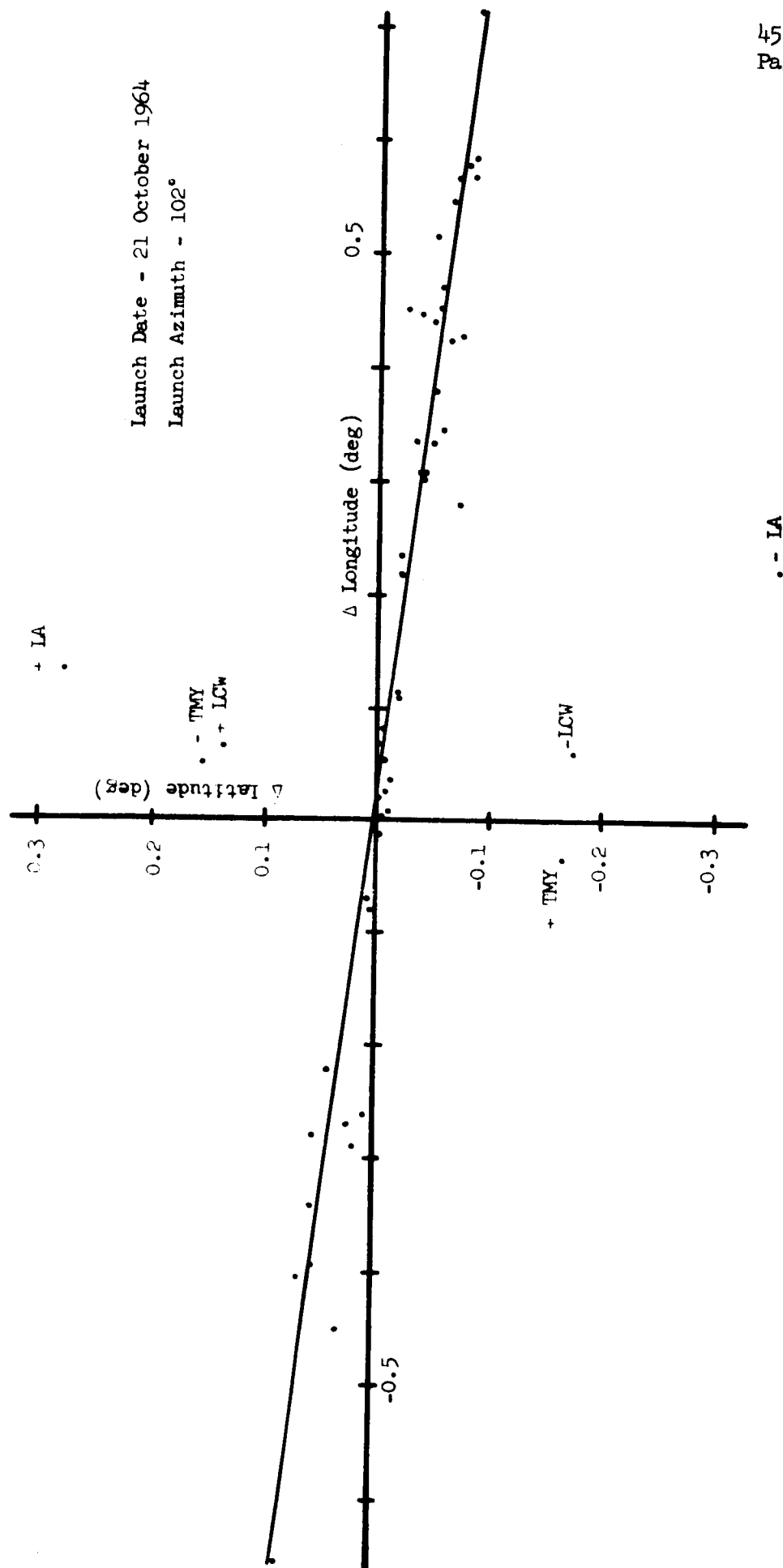
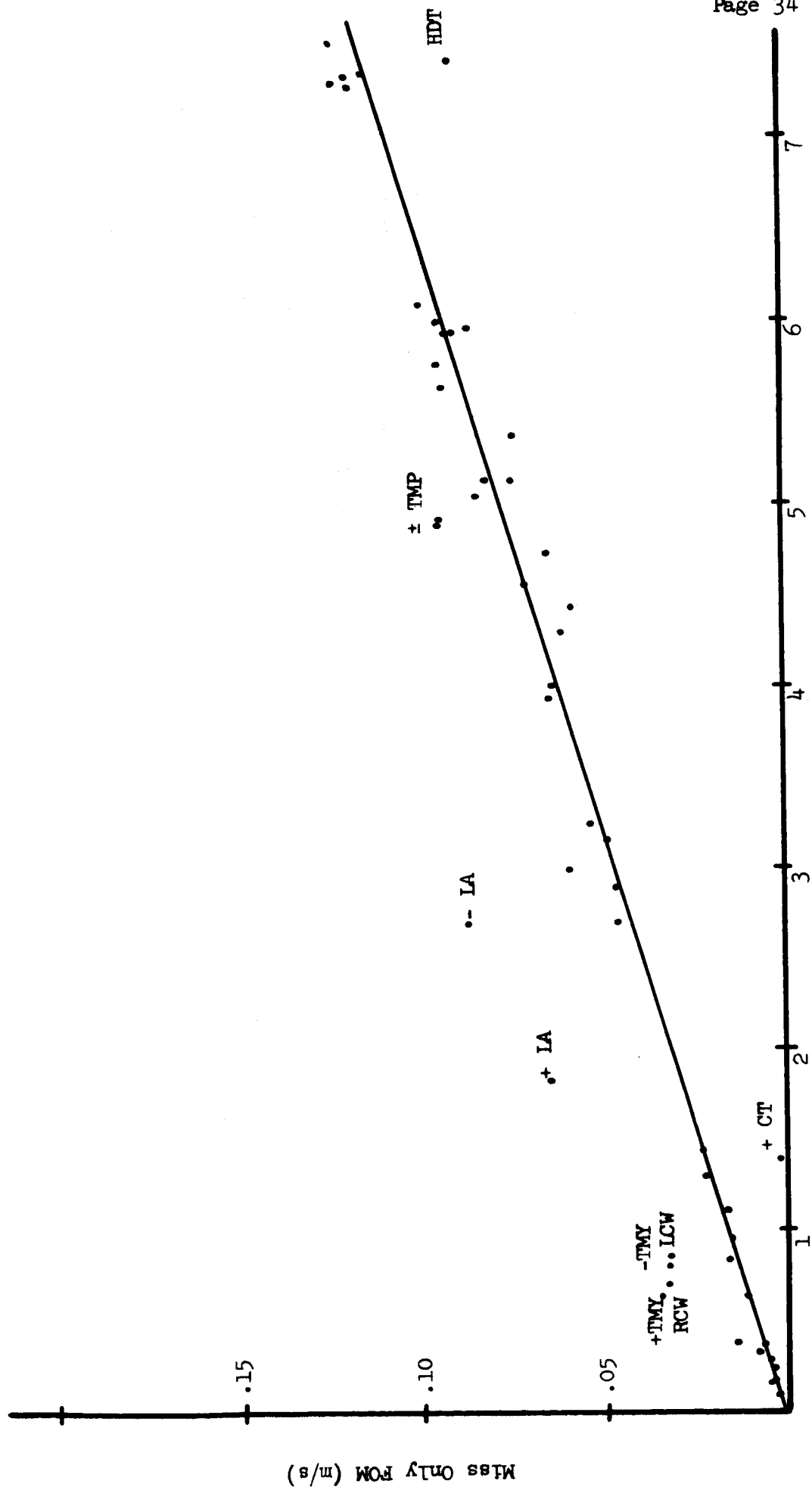


Figure 8.6 - IMPACT DISPERSIONS



Injection Energy Dispersion (1000 ft²/sec²)

Figure 8.7 - MISS ONLY FOM's vs. INJECTION ENERGY DISPERSIONS

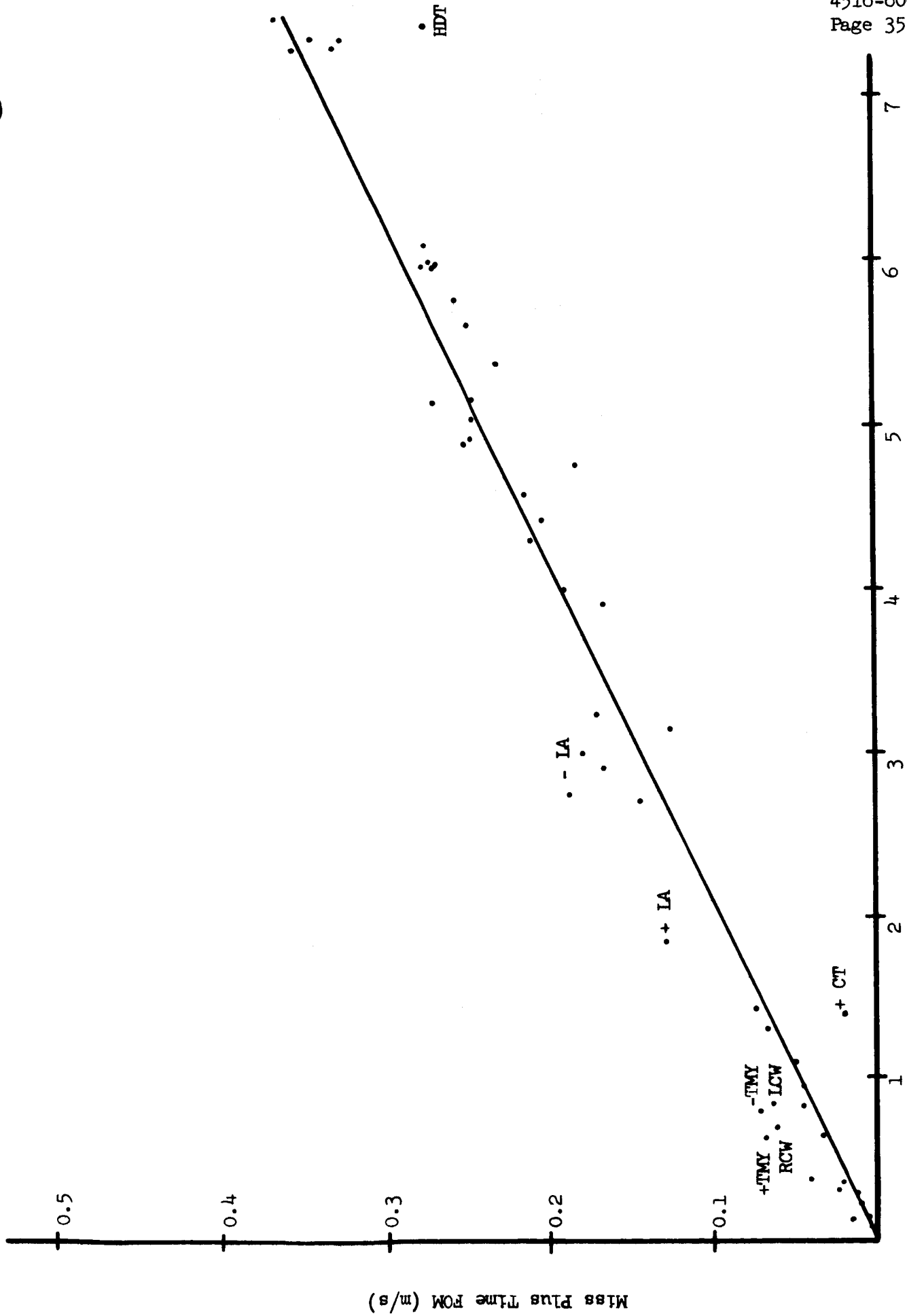


Figure 8.8 - MISS PLUS TIME FOM's vs. INJECTION ENERGY DISPERSIONS

⊙ 21 October 1964
△ 7 December 1964

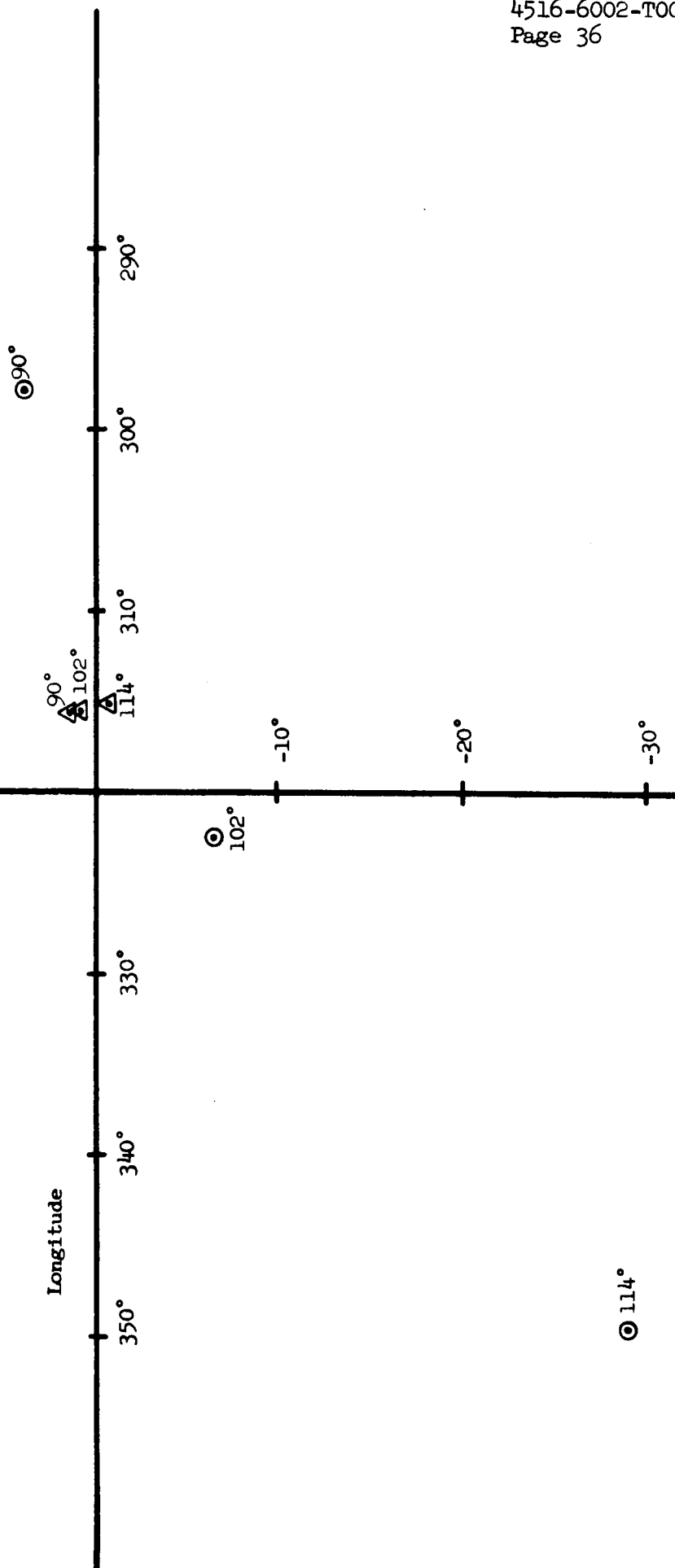


Figure 8.9 - NOMINAL IMPACT PLOT

9. CONCLUSIONS AND RECOMMENDATIONS

Based on the results presented in Section 8 and the simulation process described elsewhere, a number of conclusions can be formulated about the performance of the Two-Burn guidance equations.

9.1 Conclusions

The Two-Burn guidance equations simulated in this study exhibited no major weaknesses. Their performance under the influence of the usual perturbations was satisfactory.

The current booster pitch program (August 1965) caused excessive aerodynamic heating in this simulation.

The effect of parking orbit thrust perturbations was found to be more serious than expected. The one pound thrust perturbation simulated will cause unacceptably large impact dispersions, which completely obscure any other dispersions.

The large navigation errors encountered in a Two-Burn trajectory result in significant injection energy dispersions which contribute the largest part of the impact errors.

The form of the equations simulated is not useable for a two minute parking orbit and in fact is limited to parking orbits of more than 160 seconds duration.

The combination of yaw steering equations and gain constants used in this simulation will cause out-of-plane transients around the antipode, at the start of the second burn.

9.2 Recommendations

Magnitudes for the parking orbit thrust and drag perturbations should be established and used in future Two-Burn performance analysis.

Since the low thrust in parking orbit cannot be eliminated and the sensing errors of the accelerometers are excessive, the best method for reducing dispersions from parking orbit perturbations seems to be precise targeting. It may be possible by use of elaborate models of the atmospheric density and more detailed engine data to reduce errors from predictable effects if not from random uncertainties.

Methods for reducing the magnitude of the navigation error such as gravity biases and better integration techniques should be studied.

When the parking orbit thrust profile has been established (or at least for AC-9) the parking orbit logic should be adjusted to prevent loss of navigation data.

The use of energy-to-be-gained, ϵ , in the yaw steering equation should be re-examined in light of the step caused by the two injection energies used by the Two-Burn program.

APPENDIX A

REFERENCE TRAJECTORY

A-1 INTRODUCTION

The Two-Burn trajectory in this analysis consists of booster stage, sustainer stage, Centaur first burn, coast in a 90 n.mi. circular orbit, and Centaur second burn. A stored pitch program steers the vehicle from liftoff to booster jettison. Guidance is then employed for the remainder of the flight. The primary goal of the guidance mission is to inject the vehicle into an elliptical trajectory which will intercept the moon.

A-2 DISCRETES

The discrettes are those commands which initiate a distinct change in one of the vehicle's functions, such as an engine start or mass jettison. Those discrettes which were of importance to this analysis are described below. They were obtained from Reference 5.

- (1) Booster engine cutoff (BECO) occurs when thrust accelerations (all accelerations except gravity) reaches 5.7 g. The booster packages are then jettisoned 3.1 seconds after the BECO discrete. Booster thrust decay is simulated during this 3.1 second period by a 0.3 second period of full thrust.
- (2) Guidance control of the flight is admitted 10 seconds after BECO.
- (3) The Centaur insulation panels are jettisoned at BECO + 50 seconds, and the nose fairing at BECO + 83 seconds.
- (4) Sustainer engine cutoff (SECO) and Vernier engine cutoff (VECO) both occur at a lox depletion level of 380 lbs. or a fuel depletion level of 350 lbs. At this time, guidance steering is cut off, and the autopilot resumes attitude control.
- (5) Sustainer jettison (separation) occurs at SECO + 1.9 sec. Boost pump starting is not simulated except by weight compensations. The Centaur's main-engine prestart occurs at SECO + 3.6 sec., main engine thrust build-up (MES) starts at SECO + 8.6 sec., and the engines are at full thrust by SECO + 9.92 sec.

- (6) Guidance steering is readmitted at the time thrust buildup occurs.
- (7) The first Centaur main engine cutoff (MECO) discrete is issued by guidance when the VIS-VIVA energy has reached a predetermined value which will allow the vehicle to maintain a 90 n.mi. circular orbit. No thrust decay was simulated because the GD/C Report (Reference 1) stated that no thrust decay was used in their simulation which established the guidance constants.
- (8) The ullage engines are cutoff ((VECO)) at MECO + 120 sec by the guidance. At this time the guidance changes the navigation equations to block out sensed acceleration inputs. A four pound thrust was used for the ullage engines in this simulation since GD/C used 4 lbs. thrust throughout the parking orbit.
- (9) The main engine restart (MES) discrete is issued by guidance when the vehicle has coasted (with 4 lb. thrust) to the correct central angle from the target vector. At this time normal navigation is resumed. The 4 lb. thrust level is not changed although the weight flow allows for boost pump operation.
- (10) At MES + 46 sec. the main engine chillover is initiated by increasing the weight flow without changing thrust.
- (11) The main engine thrust buildup is begun at MES + 40 sec.
- (12) The main engines attain full thrust level at MES + 41.32 sec. Guidance steering is not locked out after the start of first burn so it is unnecessary to readmit it.
- (13) The second MECO is issued by guidance when the vehicle has reached the VIS-VIVA energy required to impact the target. No thrust decay was simulated at this MECO either.
- (14) At MECO + 60 sec. the spacecraft is separated and one second later given an axial spring kick of 0.75 ft/sec.
- (15) The simulation is switched from an earth gravity field to a linear gravity field after 3390 minutes of free flight.

A-3 NOMINAL TRAJECTORY PARAMETERS

To allow the reader a better understanding of the trajectory studied, three sets of parameters for the nominal trajectory are given:

(1) <u>Parking Orbit Injection</u>	(MECO-1)
Flight Time	569.28822 sec.
Altitude	546,995.00 ft.
Inertial Velocity	25620.69482 ft/sec.
Flight-Path-Angle	-.000448227 deg.
Orbital Eccentricity	.00082352
Apogee Altitude	96.7142 n.mi.
Perigee Altitude	90.8917 n.mi.
Orbital Period	87.86677 min.
Weight	13861.479 lbs.
(2) <u>Final Injection</u>	(MECO-2)
Flight Time	2135.6317 sec.
Altitude	21,511,702 ft.
Inertial Velocity	35911.69238 ft/sec.
Flight-Path-Angle	2.1818943 deg.
True Anomaly	4.4292629 deg.
Orbit Eccentricity	0.97087957
Apogee Altitude	235,820.0546 n.mi.
Perigee Altitude	93.8525 n.mi.
Orbital Period	17682.234 min.
Weight	6462.9374 lbs.
(3) <u>Impact</u>	
Flight Time	4.52.5856 min.
Selenographic Latitude	-6.4274584 deg.
Selenographic Longitude	322.3956832 deg.
Impact Velocity	8506.457275 ft/sec.
Impact Angle	166.52024 deg.

APPENDIX B

VEHICLE MODEL

B-1 INTRODUCTION

A vehicle model is required for the general vehicle dynamics simulation. Specific data for the model used are presented in the following paragraphs.

B-2 MASS PROPERTIES

Mass values were obtained from Reference 5. A liftoff mass of 302,306 lb. is used. During the Atlas sustainer burn, a 7292 lb. booster engine, 1285 lb. insulation panels and a 1799 lb. nose fairing are jettisoned at the appropriate times. After separation, the Centaur plus payload mass is 36,521 lb.

Tables of CG versus mass were obtained from the TRW Weights Group in January 1964 (Reference 6) and have not been updated. The pitch moment-of-inertial tables were prepared by the same group and used for both pitch and yaw in the vehicle model.

B-3 PROPULSION SYSTEM

B-3.1 Atlas Propulsion

A detailed Atlas propulsion model using the data in propulsion section of Reference 6 is used. This model has the two booster engines of 165,000 lb. thrust each and a sustainer engine rated at 81,000 lb. thrust at sea level.

The booster engine thrust decay (cutoff impulse) is simulated by biasing the BECO discrete to cutoff 0.3 sec. late. Then all discrettes biased on BECO time are shifted by this amount.

B-3.2 Centaur Propulsion

The Centaur propulsion model is simply a constant thrust of 30,000 lb. and a constant propellant flow of 69.3 lb./sec. A detailed propulsion model is available (Reference 7). However, the simplified propulsion model should be adequate for the purposes of this study.

Thrust buildup is approximated by simulating starting impulses equivalent to the values found in Reference 6.

B-4 AERODYNAMIC PROPERTIES

The TRW general vehicle dynamics simulation contains the Patrick AFB atmospheric model up to an altitude of 302,000 ft. Above this altitude, aerodynamic computations are bypassed in the simulation. Therefore the longitudinal and normal force coefficients and center-of-pressure location tables are used only during Atlas booster and sustainer powered flight. These data may be obtained from Reference 8.

B-5 VEHICLE DIMENSIONS

For aerodynamic purposes the cross-sectional area of the vehicle is 78.5 sq. ft. All locations in the vehicle longitudinal direction are specified by station number, the distance between two consecutive station numbers being 1 inch. The Atlas-Centaur engine gimbals station was set at 1212. The Centaur vehicle engine gimbals station is 453.

B-6 GEOPHYSICAL DATA

B-6.1 Atmospheric Model

The Patrick AFB atmospheric model (Reference 8) was used in the vehicle dynamics simulation.

B-6.2 Gravity Model

The earth gravity model is obtained from Reference 9.

B-6.3 Launch Site

Astronomic Latitude	28.47117996 deg.
Geodetic Latitude	28.47158288 deg.
Launch Altitude	49.195 ft.*
Geoidal Separation	-101 ft.**
Longitude	-80.53824138 deg.

B-6.4 Miscellaneous Constants

Gravitational Constant	$0.14076539 \times 10^{17} \text{ ft}^2/\text{sec}^2$
Average Radius of Spheroid	20,925,738.25 ft.
One n. mi.	6076.103271 ft.
One Kilometer	.0003048 ft. (exact)
Earth Rotation Rate	$.72921152 \times 10^{-4} \text{ rad/sec}$

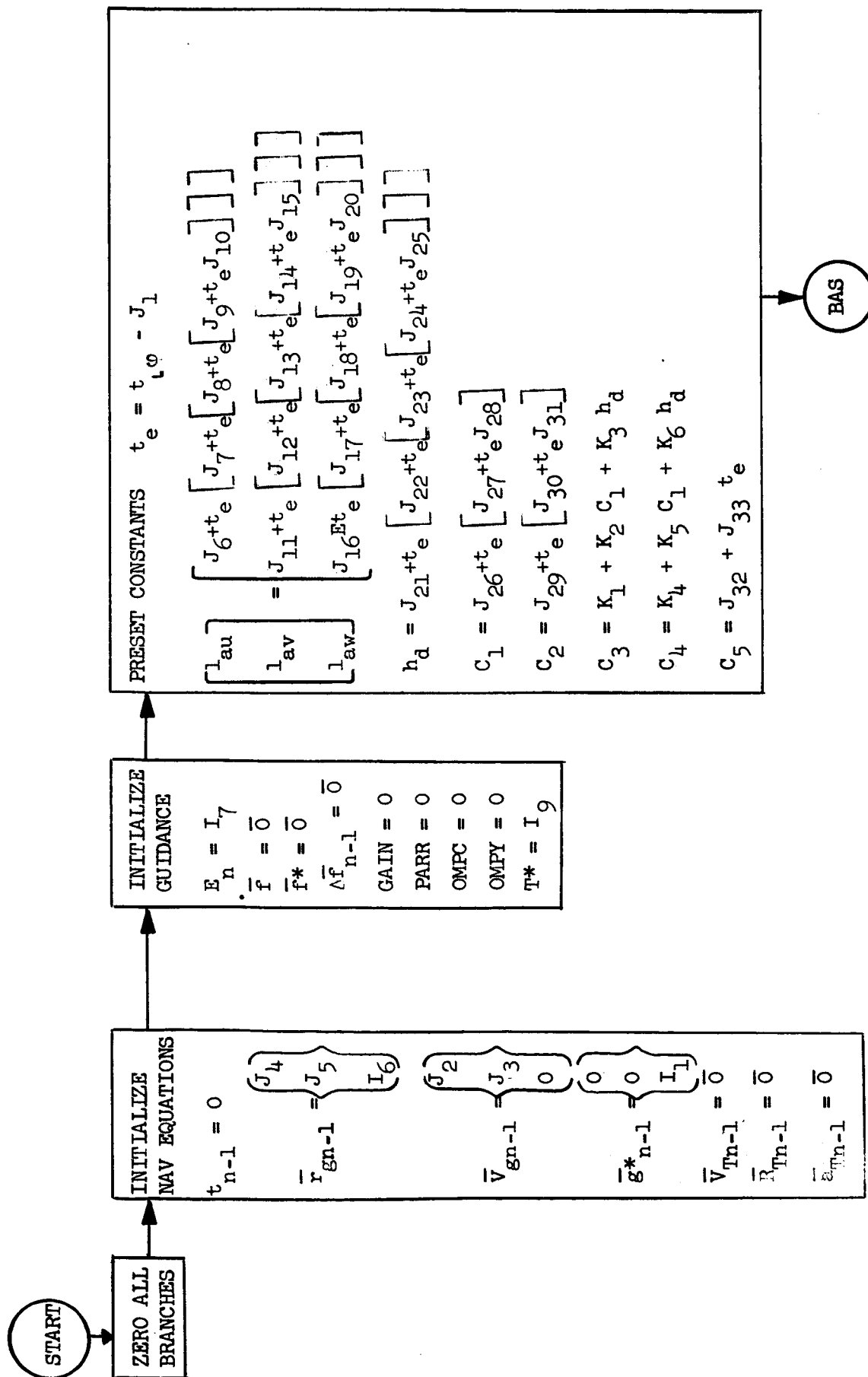
* Altitude of the launch pad above mean sea level.

** Geoidal separation is the altitude of mean sea level above the reference ellipsoid.

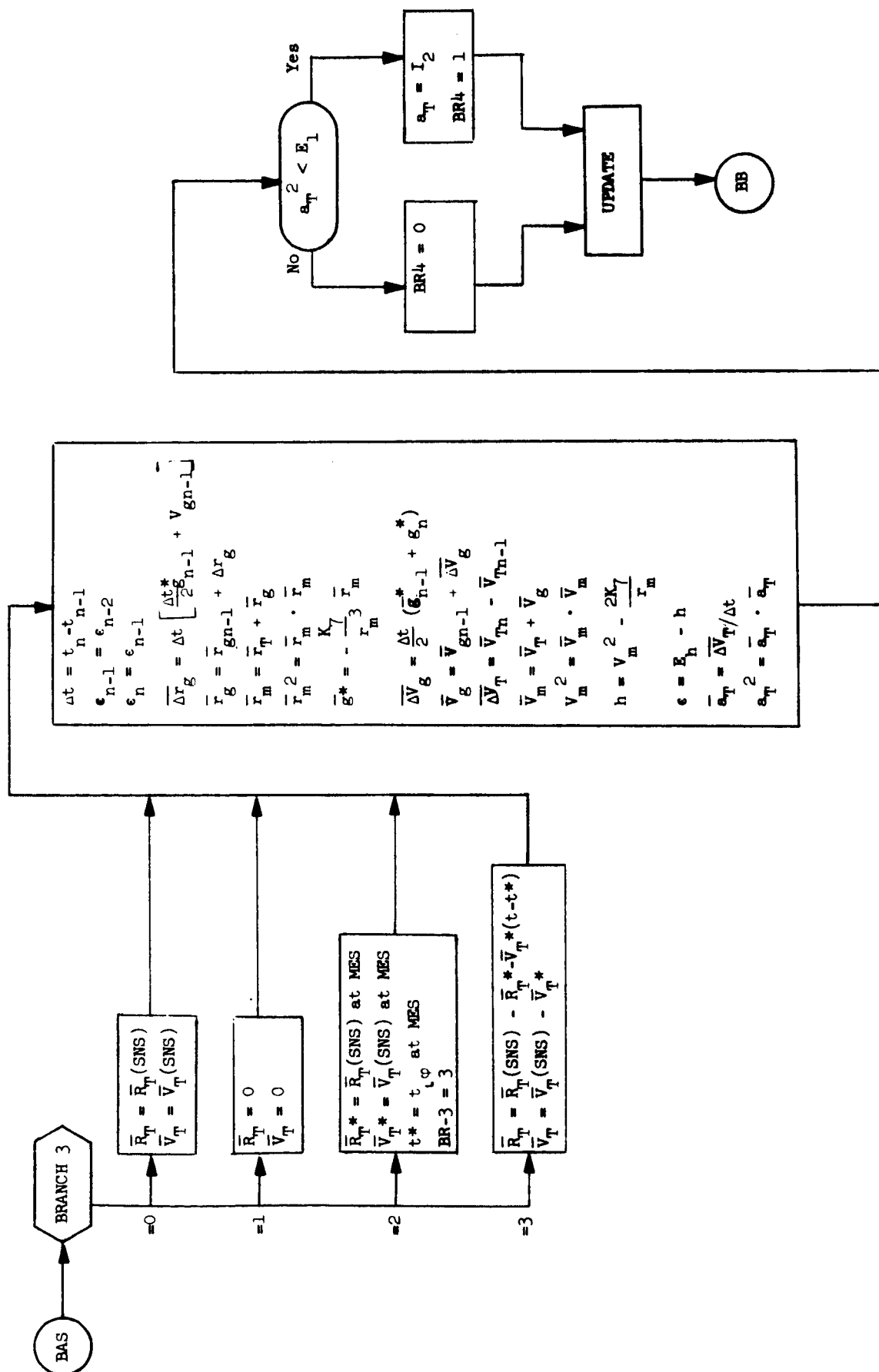
APPENDIX C

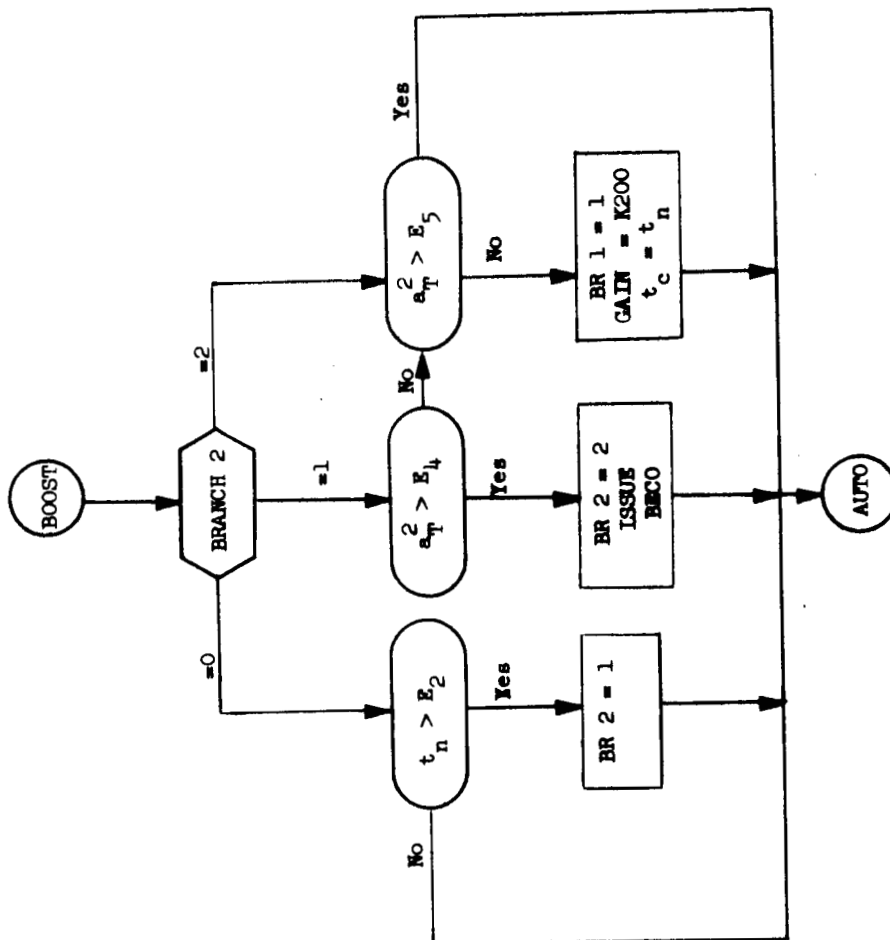
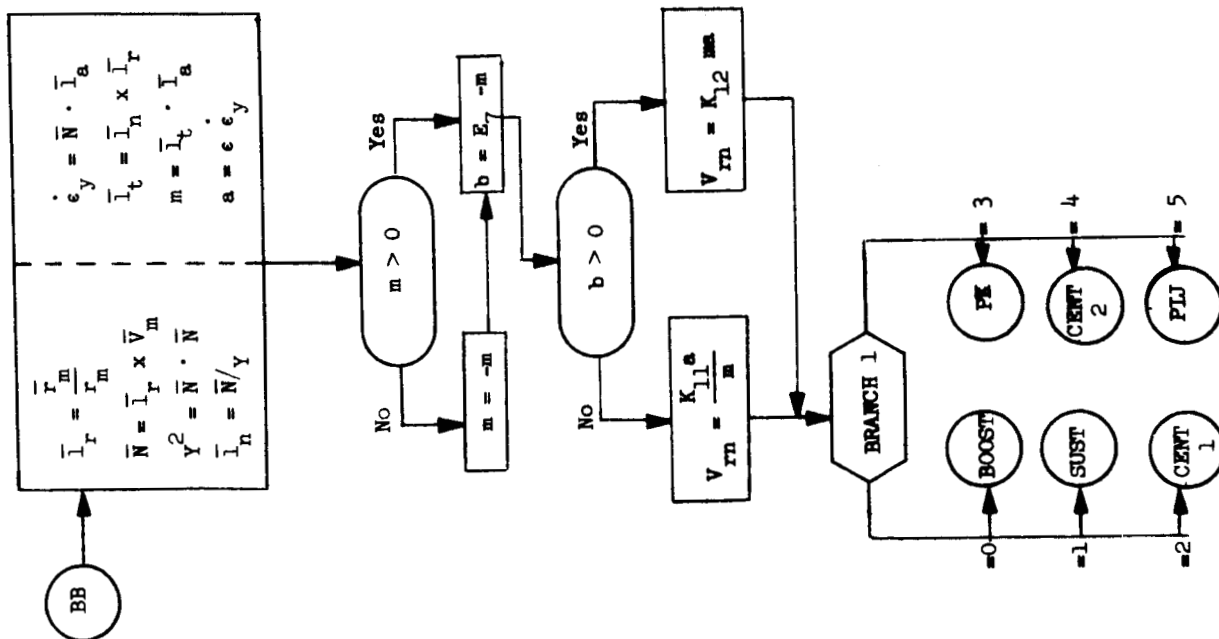
TWO-BURN GUIDANCE EQUATION FLOW CHARTS

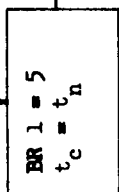
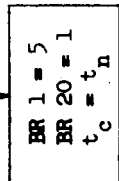
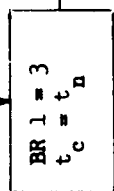
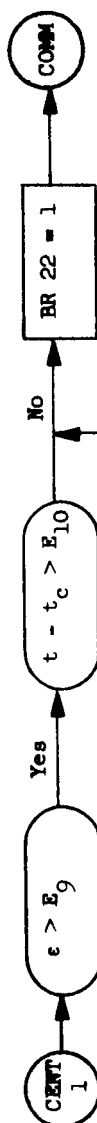
The following flow charts represent the Two-Burn guidance equations as programmed for this performance analysis. The significant differences from those given by GD/C in Reference 1 are outlined in Section 4 of this report.

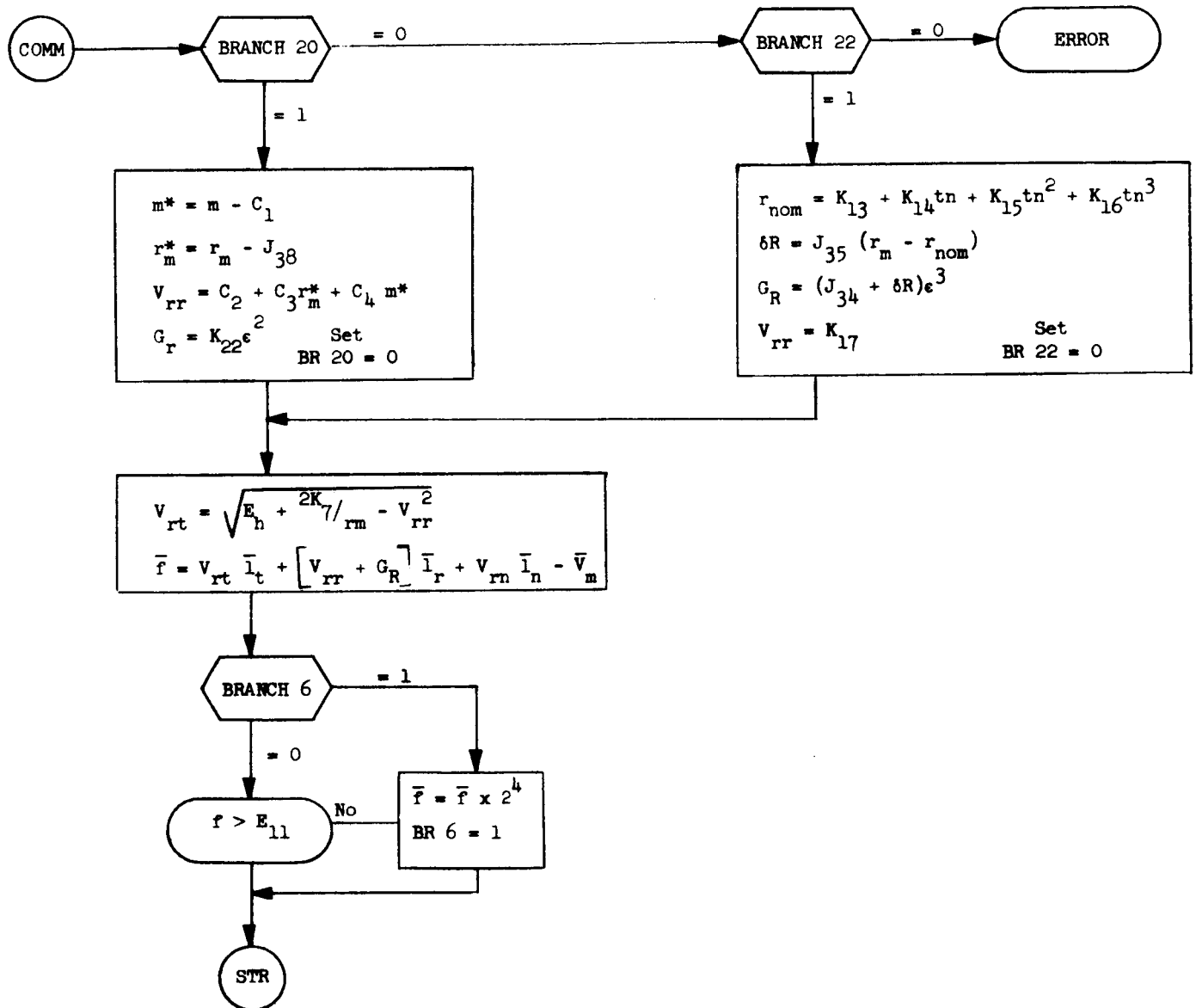


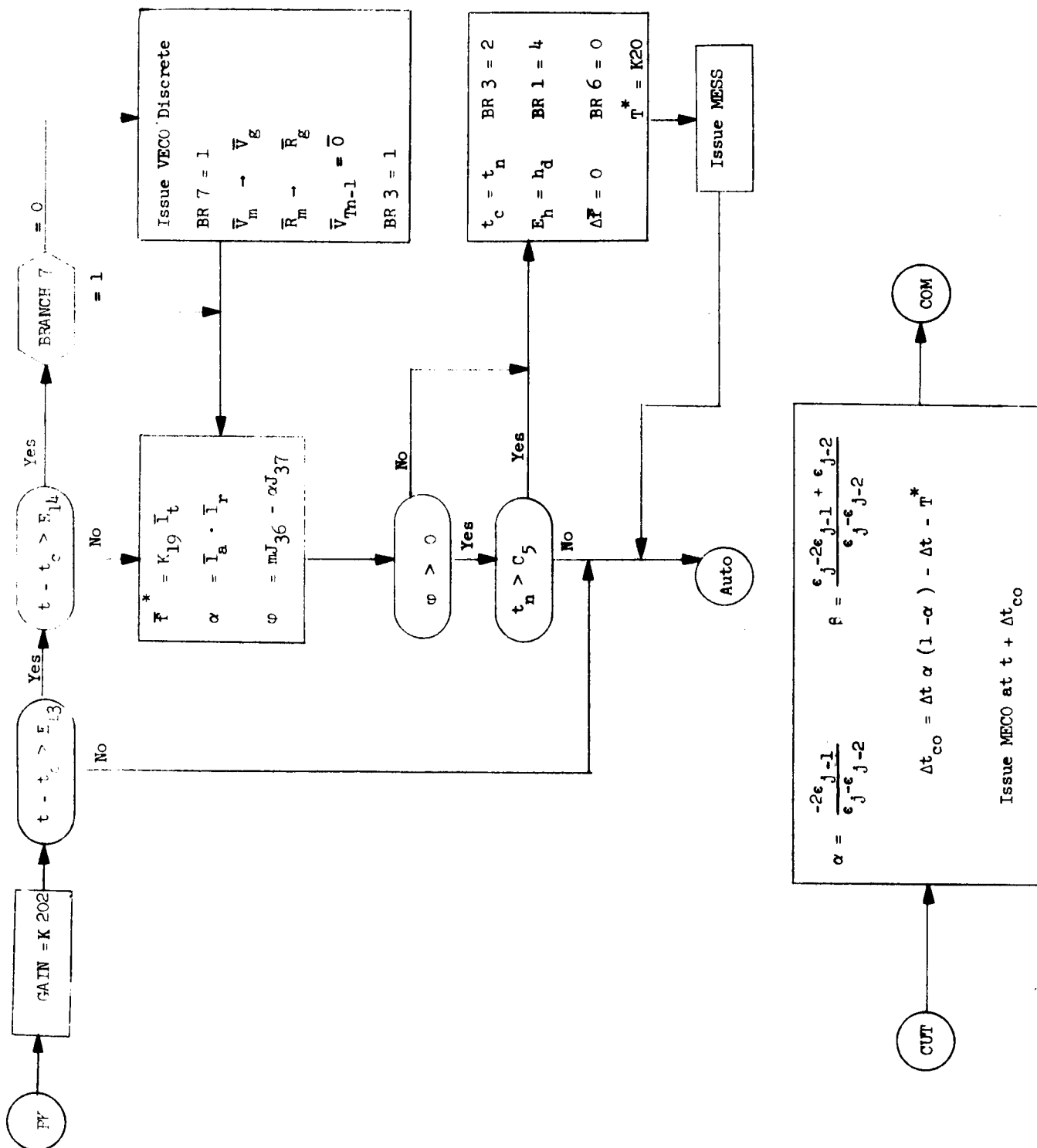
New Equations - Two Burn AC-8 - STL Version of GDC Equation of 12 May 1965
Incorporated in SNS Program identified as Modified Equation.

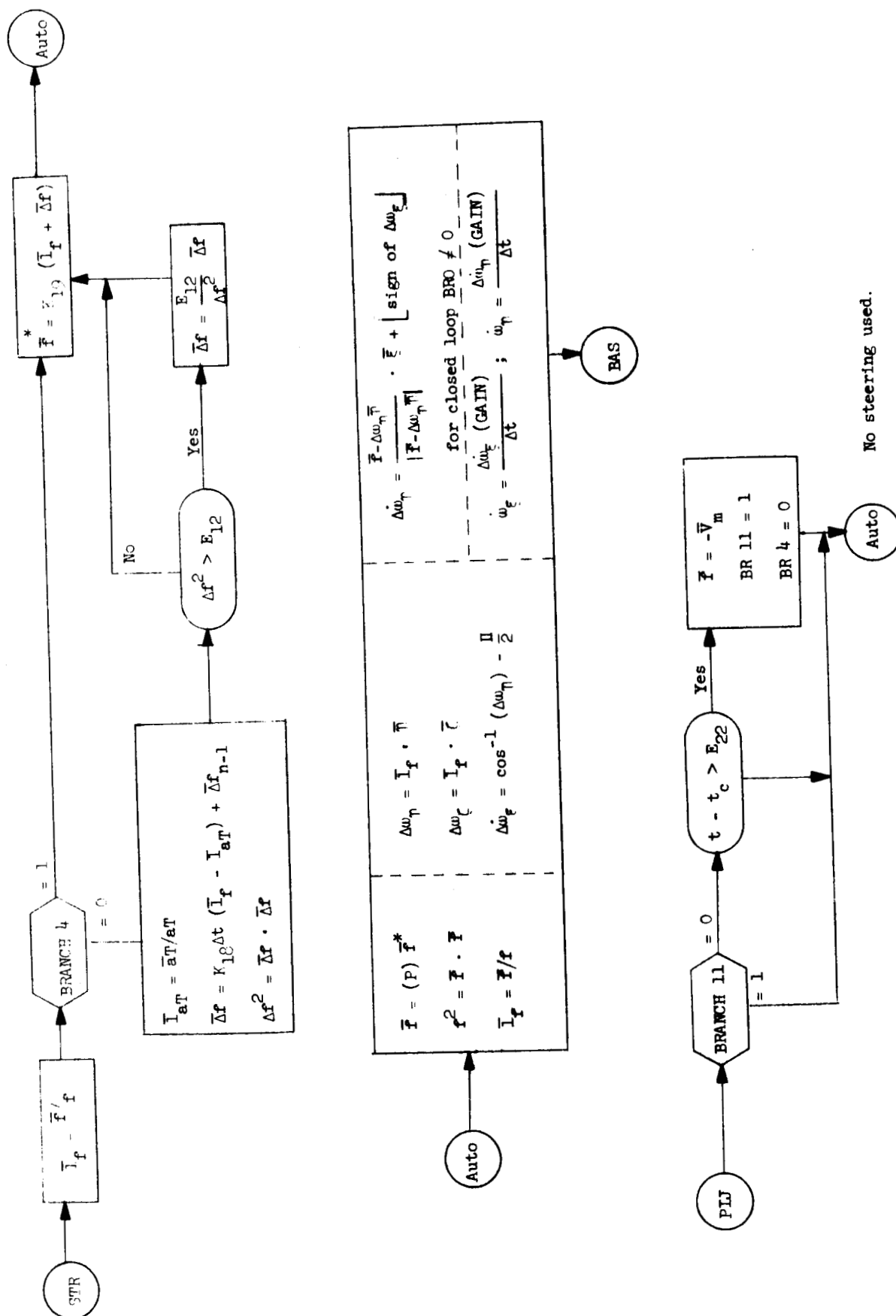












REFERENCES

1. K.G. Cameron, "Preliminary Guidance Equations for Surveyor Parking Orbit Ascent Mode", Dated 1 April 1965, GD/C Report No. BTD65-033.
2. R.E. Roberts, "Final Guidance Equations and Performance Analysis for Centaur AC-7", Dated 11 June 1965, GD/C Report No. BTD65-096.
3. K.G. Cameron, "AC-8 Guidance Equations", Dated 19 May 1965, GD/C Flow Charts.
4. T.J. Pavlick, "Atlas/Centaur Performance Dispersions - Description, Usage and Data - Flights AC-6 and On", Dated 23 April 1965, GD/C Report No. BTD65-057.
5. A.E. Hunt, "Centaur Monthly Configuration Performance and Weight Status Report", Dated 21 November 1964, GD/C Report No. GDA63-0495-18.
6. J.G. Reid, "Centaur Data Handbook", (Confidential), Dated January 1964, TRW Report No. 8414-6020-RC000.
7. F.C. Gray, "Simulation of the Centaur Propulsion System", Dated November 1963, TRW Document No. 8414-6137-RC000.
8. O.E. Smith, "A Reference Atmosphere for Patrick AFB, Florida", Dated March 1961, NASA Technical Note No. TN-D-595.
9. V.C. Clark, Jr., "Constants and Related Data Used in Trajectory Calculations at the Jet Propulsion Laboratories", Dated 1 May 1962, JPL Technical Report No. 32-273.

DISTRIBUTION

W. J. Beil (15)
R. Braslau
H. D. Culver (2)
F. T. Cummings
R. P. Davis
A. A. Dzilvelis (3)
W. J. Hindman Jr.
W. K. Hrushow